Geoderma Regional 35 (2023) e00715

Contents lists available at ScienceDirect

Geoderma Regional

journal homepage: www.elsevier.com/locate/geodrs

# Archaeopedological reconstruction of Middle Bronze Age subsistence farming in SW-Germany from sedimentary archives in the Western Allgäu

Sascha Scherer [a,b,*], Benjamin Höpfer [b,c], Katleen Deckers [d], Markus Fuchs [e], Ellen Kandeler [f], Eva Lehndorff [g], Johanna Lomax [e], Sven Marhan [f], Christian Poll [f], Wroth Kristen [h], Thomas Knopf [b,i], Thomas Scholten [b,j], Peter Kühn [b,j]

[a] University Mainz, Department of Geography, Johann-Joachim-Becher-Weg 21, 55099 Mainz, Germany
[b] University Tübingen, SFB1070 ResourceCultures, Gartenstraße 29, 72074 Tübingen, Germany
[c] Canton Aargau, Archaeological Service, Industriestrasse 3, 5200 Brugg, Switzerland
[d] University Tübingen, Institute for Archaeological Sciences, Hölderlinstraße 12, 72070 Tübingen, Germany
[e] University Gießen, Department of Geography, Senckenbergstraße 1, 35390 Gießen, Germany
[f] University of Hohenheim, Institute of Soil Science and Land Evaluation, Emil-Wolff-Straße 27, 70593 Stuttgart, Germany
[g] University of Bayreuth, Department of Biology, Chemistry and Geosciences, Dr.-Hans-Frisch-Straße 1-3, 95448 Bayreuth, Germany
[h] Earlham College, Department of Chemistry, 801 National Road West, Richmond, IN 47374, USA
[i] Celtic Museum Hochdorf/Enz, Keltenstraße 2, 71735 Eberdingen-Hochdorf, Germany
[j] University Tübingen, Department of Geosciences, Rümelinstraße 19-23, 72070 Tübingen, Germany

ARTICLE INFO

*Keywords:*
Archaeopedology
Multi-proxy analysis
Colluvial archives
Subsistence farming

ABSTRACT

In the northern Alpine foreland, there was a shift at the transition from the Early Bronze Age (EBA, 2200–1600 BCE) to the Middle Bronze Age (MBA, 1600–1250 BCE). This shift was associated with a widespread abandonment of the pile-dwelling settlements around the pre-Alpine lakes and an expansion and intensification of low- and mid-altitude inland settlements. A research gap exists regarding the nature of MBA subsistence in these inland areas, which are considered unfavourable for agriculture.

We analysed multi-layered colluvial and alluvial deposits in the agriculturally unfavourable Western Allgäu region to gain insights into MBA subsistence farming. Phases of deposition were determined by optically stimulated luminescence (OSL) technique and AMS radiocarbon ($^{14}$C) measurements of charcoal. They provide a chronostratigraphic framework that is correlated to the local archaeological record. Subsistence farming was reconstructed using land use proxies such as phytoliths, charcoal spectra, urease activity to microbial biomass carbon ($C_{mic}$) ratios, faecal biomarkers, polycyclic aromatic hydrocarbons (PAHs) and heavy metals.

The OSL and $^{14}$C ages indicate phases of deposition and land use during the MBA. They correlate with two recently excavated MBA inland settlements in the Western Allgäu. Human-induced vegetation change promoted open woodland comprising of *Juniperus* and *Quercus* at the expense of *Abies* and *Fagus*. The accumulation of charcoal and PAHs in MBA related colluvial horizons is most likely associated with the use of fire to maintain an open landscape. Partially increased urease activity to $C_{mic}$ ratios and the appearance of *Juniperus* indicate the importance of livestock farming within the MBA subsistence.

Our results show that there was an extensive and diversified subsistence economy in the Western Allgäu during the MBA. They thus reflect an adaptation of MBA farmers to the harsher climatic conditions of the Western Allgäu, where crop yields were certainly less predictable than, for example, in regions near Lake Constance.

## 1. Introduction

The success of prehistoric agriculture was closely related to environmental resources such as soil quality, climate, elevation and relief (James et al., 2021; McNeill and Winiwarter, 2004). In general, it was assumed that areas favourable for agriculture, i.e. with loess cover,

* Corresponding author at: University Mainz, Department of Geography, Johann-Joachim-Becher-Weg 21, 55099 Mainz, Germany.
*E-mail address:* saschere@uni-mainz.de (S. Scherer).

https://doi.org/10.1016/j.geodrs.2023.e00715
Received 9 June 2023; Received in revised form 6 September 2023; Accepted 23 September 2023
Available online 28 September 2023
2352-0094/© 2023 The Authors. Published by Elsevier B.V. This is an open access article under the CC BY license (http://creativecommons.org/licenses/by/4.0/).

low elevation and low relief intensity were settled first (Bogaard et al., 2013; Ryzner and Owczarek, 2020), while areas with lower soil quality, higher elevation and steeper relief were avoided for subsistence farming. Progress in agricultural technology and management (e.g., ploughing, crop diversity) allowed farmers to settle in both agriculturally favourable and unfavourable areas (Harding, 2000; Miera, 2020; Tinner et al., 2003).

To date, little is known about Middle Bronze Age (MBA, 1600–1250 BCE) subsistence such as arable and livestock farming and forest management in agriculturally unfavourable areas in the northern Alpine foreland. These areas are often located in the low- and mid-altitude inland, where the absence of lacustrine sediments leads to weaker preservation of biogeochemical and archaeobotanical proxies as well as archaeological structures in soils (Jansen and Wiesenberg, 2017; Vogt and Kretschmer, 2019). However, recent progress in colluvial research has shown that specific land use proxies such as biomarkers are well archived in colluvial soils as they are preserved by repeated sedimentation and low microbial turnover in greater soil depth (Kaal and Mailänder, 2019; Kühn et al., 2017; Zádorová et al., 2015). Multi-layered colluvial soils within an archaeological context have the potential to provide insights into the location of ancient farmlands as well as associated subsistence practices and vegetation changes, even in agriculturally unfavourable areas. In this way, small-scale subsistence strategies of prehistoric societies can be reconstructed in combination with the local archaeological record (Ponomarenko et al., 2020; Scherer et al., 2021a; Teuber et al., 2022).

The northern Alpine foreland is roughly divided into areas more favourable for prehistoric agriculture around the larger lakes (e.g., Hegau region) and areas unfavourable for prehistoric agriculture in the low- and mid-altitude inland. From a lakeshore perspective, there was a shift at the transition from the Early Bronze Age (EBA, 2200–1600 BCE) to the MBA, leading to far reaching land abandonment and inland migration. This turn away from lacustrine habitats is often explained with the Löbben climatic depression presumed to span most of the MBA (Menotti, 2009). However, a re-dating of the Löbben oscillation into the EBA indicates a climatic optimum during the MBA (Maise, 2022). Either way, the shifting settlement distribution caused MBA sedimentation phases beyond the lakes due to an intensification of land use activities (Höpfer et al., 2016; Scherer et al., 2021b). While the lakeshore areas have been frequently studied, there is little information on MBA subsistence farming in inland areas (Menotti, 2003). The Western Allgäu can be seen as an archetypal example of a supposedly unfavourable area for prehistoric subsistence in the northern Alpine foreland, distant from the larger pre-Alpine lakes and with higher elevation and precipitation.

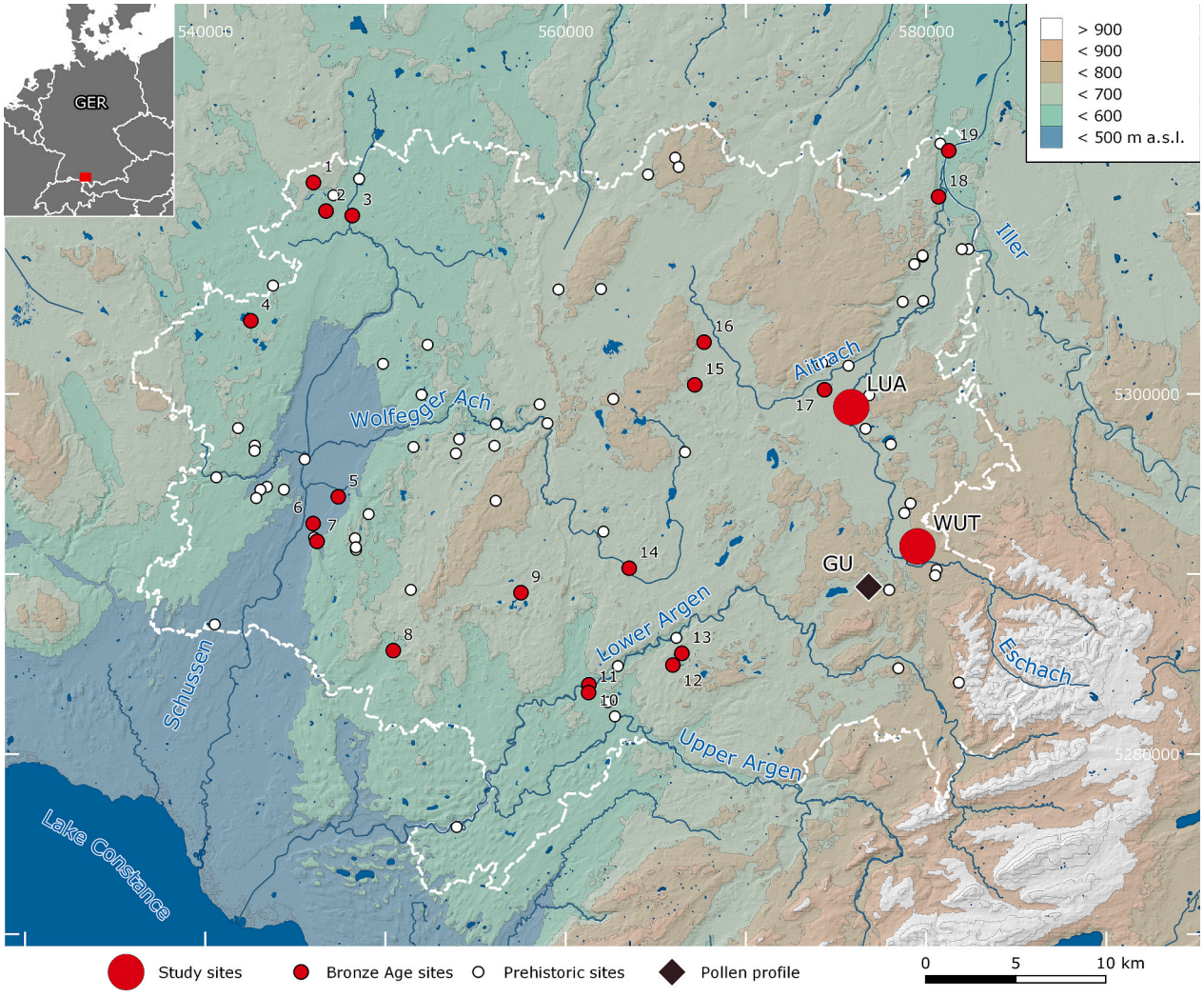


**Fig. 1.** Study area (Western Allgäu, SW-Germany) with the two Middle Bronze Age study sites "Leutkirch Untere Auen" (LUA) and "Winterstetten Urlauer Tann" (WUT), the pollen profile of "Lake Großer Ursee" (GU) and further Bronze Age and chronologically non-specified prehistoric sites (see also Table S6). Coordinates are shown in UTM 32 N reference system (EPSG 25832). Image credits: DEM "NASA SRTM-1 V.3" © NASA JPL, NASA Shuttle Radar Topography Mission Combined Image Data Set. NASA EOSDIS Land Processes DAAC (2014), https://doi.org/10.5067/MEaSUREs/SRTM/SRTMIMGM.003; offical water management network © Landesanstalt für Umwelt Baden-Württemberg (2020), https://udo.lubw.baden-wuerttemberg.de.

Human activity in the Western Allgäu has been documented since the Neolithic, albeit rather scarcely and often in the form of stray finds (Mainberger et al., 2020). Vogt (2015) identified phases of intensive colluviation during the EBA near Lake Degersee, one of the few larger lakes in the Western Allgäu lowlands. While this colluviation can certainly be associated with agricultural activities, it remains unclear how far it is representative of the Western Allgäu in general or more a continuation of lake dwelling tradition during the EBA. Based on a pollen profile in the Western Allgäu inland (Fig. 1), Rösch et al. (2020) concluded only weak human impact during the MBA and showed intense human activity in the form of cereal cultivation not before the late pre-Roman Iron Age (Latène Period, 450 BCE – 0). These results of early human activity in the Western Allgäu contrast with a number of recently excavated MBA settlement sites, suggesting a frequent occupation of the Western Allgäu during the MBA (Höpfer et al., 2020; Morrissey et al., 2021). These settlement sites are therefore an excellent setting to study MBA subsistence farming in supposedly agriculturally unfavourable areas. In this study, we focus on the reconstruction of MBA subsistence practices from colluvial and alluvial soils in the Western Allgäu (SW-Germany) and hypothesize that:

i. there was substantial subsistence farming (e.g., arable and livestock practices, forest management) in the vicinity of MBA sites in the Western Allgäu (SW-Germany). If this is the case, it can be expected that there were perennial rural settlements in the low- and mid-altitude inland of the northern Alpine foreland, which were previously considered unfavourable for subsistence farming;
ii. due to the environmental resources, subsistence practices had to be adapted in the Western Allgäu. Therefore, the subsistence practices derived from colluvial and alluvial soils in the Western Allgäu differ from subsistence strategies known from areas more favourable for agriculture (e.g., Hegau region).

To address the hypotheses, we used an archaeopedological analysis of multi-layered colluvial and alluvial soils near MBA settlements. Phases of colluvial deposition were dated by optically stimulated luminescence (OSL) techniques and AMS radiocarbon ($^{14}C$) measurements of charcoal to provide a chronostratigraphic framework that can be correlated with the local archaeological records. The analysis of the soil microstructure was used to confirm the colluvial stratigraphy and to prove soil tillage. Land use proxies such as phytoliths, charcoal spectra, urease activity to microbial biomass carbon ($C_{mic}$) ratio, faecal biomarker, polycyclic aromatic hydrocarbons (PAHs) and heavy metals were used to gain insights into the MBA subsistence farming.

## 2. Study area

### 2.1. Landscape setting

As part of the northern Alpine foreland, the Western Allgäu is located north-east of the Lake Constance basin (Fig. 1). The present landscape was mainly shaped by the eastern Rhine valley glacier and is characterized by glacial relief forms such as drumlins, ground and terminal moraines as well as by lakes and bogs that developed after the glacier's retreat (Scholz, 2016). Geologically, the glacial and fluvioglacial sediments of the Würm glaciation dominate. The sediments of the Riss glaciation (Donau-Iller-Lech Platte) and the upper freshwater molasse (upper tertiary) are restricted to the northern and eastern part of the study area (Geyer et al., 2011). Glacial tills, which originated from the northern (calcareous) and central (crystalline) Alps, are the soil substrate with varying amounts of gravel, sand and silt. Cambisols, Luvisols, Stagnosols and Calcaric Regosols, which developed from the glacial deposits, dominate the Reference Soil Groups according to IUSS Working Group WRB (2015) (Fig. S1). On average, elevation is 650–700 m a.s.l., mean annual temperature is 6–7 °C and precipitation is 1200 mm. The natural vegetation mainly consists of *Fagus*, with a subdominance of *Abies* and *Picea* (Müller et al., 1974).

The study site "Leutkirch Untere Auen" (LUA) is situated in the eastern part of the study area and located on a smooth area built of lower terrace gravel deposits of the Rhine valley glacier (in average 650 m a.s.l., Fig. 2). The colluvial/alluvial profiles are in the floodplain area of the Eschach river with varying influence of alluvial loam and eroded glacial till. The profile LKTT 1 is in a paleochannel of the Eschach river and developed from the sediments of the lower terrace gravel deposits. Soil formation dominantly led to Cambisols with weak and areal clay illuviation. The profiles are in the surrounding area of an MBA settlement (Fig. 2, in red, green) (see subchapter 2.2).

The study site "Winterstetten Urlauer Tann" (WUT) is in the eastern part of the study area. The archaeological finds are located on a moraine hill of the Riss glaciation (715 m a.s.l.) that covers an accumulation of tertiary freshwater molasse. The colluvial profiles WUT GS1 and WUT GS2 are at the eastern edge of the floodplain area of the Eschach river (Fig. 3). The colluvial profiles showed varying amounts of sediments of the upper freshwater molasse and glacial till. The profiles WUT WG1 and WUT WG3 are within an MBA rampart-ditch-structure and developed from anthropogenically relocated Riss moraine soil material with weak podzolic features. The profiles and archaeological finds are part of an MBA settlement complex consisting of a hilltop and a valley settlement, burial mounds and a rampart-ditch-structure (see subchapter 2.2).

### 2.2. Archaeological and palaeobotanical setting

The Western Allgäu has never been a hotspot of archaeological investigations, so the state of research concerning its prehistory is poor (Mainberger et al., 2020; Morrissey et al., 2021). Many archaeological sites in the study area can only be classified vaguely as prehistoric, being unexcavated ramparts, burial mounds or unspecific stray finds. Nonetheless, at least 23 Bronze Age sites are known, and 19 of them can still be localized with sufficient precision (Höpfer, 2020; Fig. 1). Along with the majority of undated sites, their distribution can be related to the larger water ways, especially the Schussen and Wolfegger Ach in the west, the Upper and Lower Argen in the southeast and the Eschach and Aitrach in the northeast. The EBA is mostly represented by isolated copper or bronze artefacts like axes and rings, whereas settlement or burial sites are only known from the very latest EBA and the transition to the MBA. Settlements as well as burial sites are regularly known in this region from the MBA until the LBA. Hence, the sparse archaeological data that is currently available seems to attest for an intensification of land use in the Western Allgäu since the 17th or 16th century BCE, even if it remains unclear whether this should be seen as a gradual process or as a rather prompt colonisation.

Of the few pollen records in the Western Allgäu investigated so far, the south-easternmost is Lake Großer Ursee, ca. four kilometres south-west of the WUT site and ten kilometres south of the LUA site (Fig. 1). The pollen profile represents nearly complete Late Würmian and Holocene sequences with sufficient pollen preservation (Rösch et al., 2020). *Fagus* and *Abies* dominated the woodlands of the Atlantic period and further established during the Subboreal. First phases of weak human impact were identified in the Early (~ 4500 BCE) and in the Final Neolithic (~ 2500 BCE) as indicated by an increase in crop weed (*Plantago lanceolata, Rumex, Arte misia*) and cereal pollen (*Triticum-type, Hordeum-type*) as well as by moderate decline in *Fagus*. Based on the pollen record of Lake Großer Ursee, substantial human impact first occurred during the pre-Roman Iron Age (Latène Period, 475–15 BCE) and led to considerable clearances of the dense *Fagus* woodlands, which continued during the Roman and Medieval Periods (Rösch et al., 2020; Tserendorj et al., 2021).

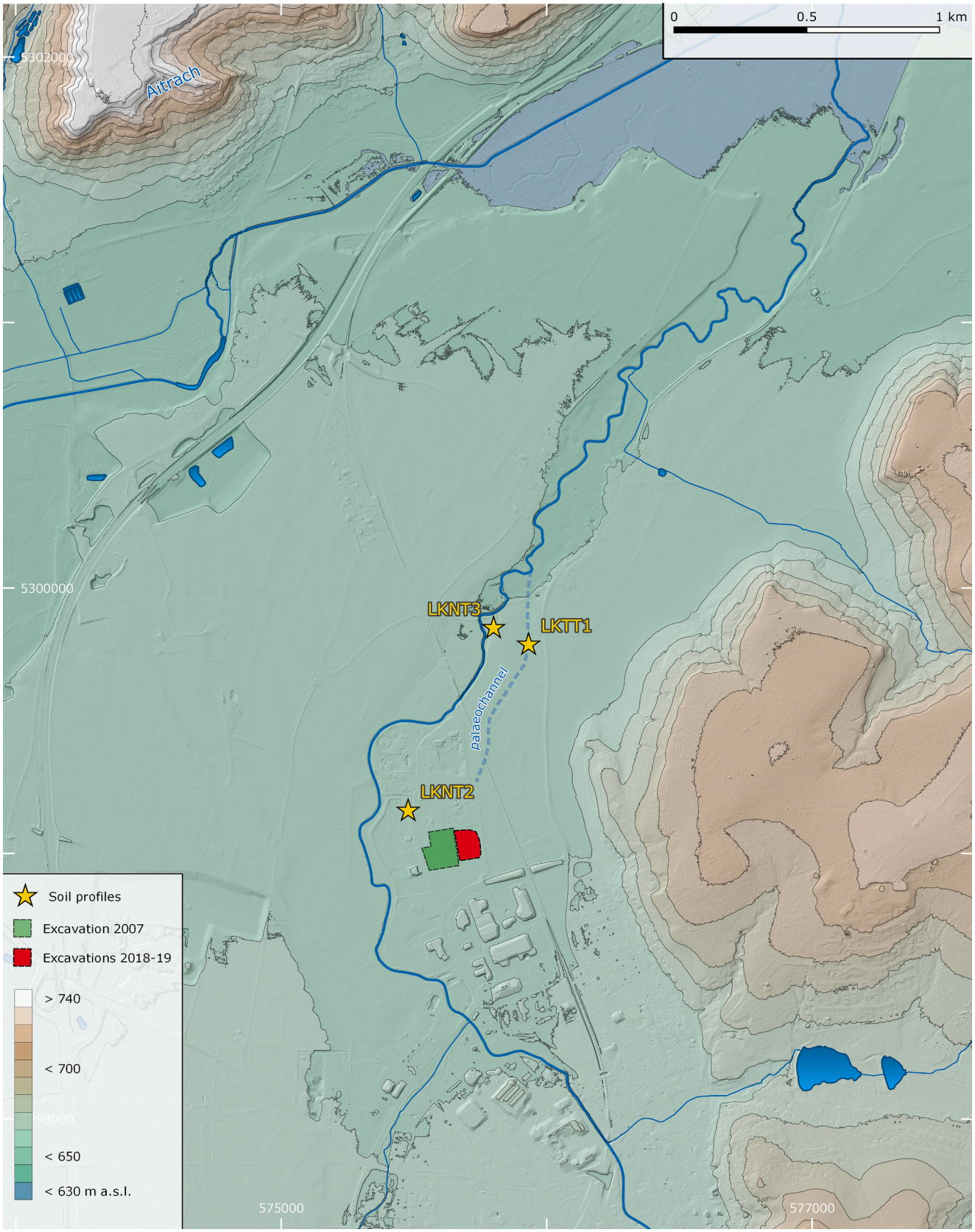


**Fig. 2.** Study site of "Leutkirch Untere Auen" (LUA) with the Middle Bronze Age settlement (area in red, green) site and colluvial profiles (yellow stars) and their topographic situation. Coordinates are shown in UTM 32 N reference system; EPSG 25832. Image Credits: LiDAR-DEM (resolution 1 × 1 m, captured in 2002, © LGL Baden-Württemberg, www.lgl-bw.de, Az.: 2851.9–1/19) and official waterway network «AWGN» (© Landesanstalt für Umwelt Baden-Württemberg, downloaded in May 2020 from https://udo.lubw.baden-wuerttemberg.de).

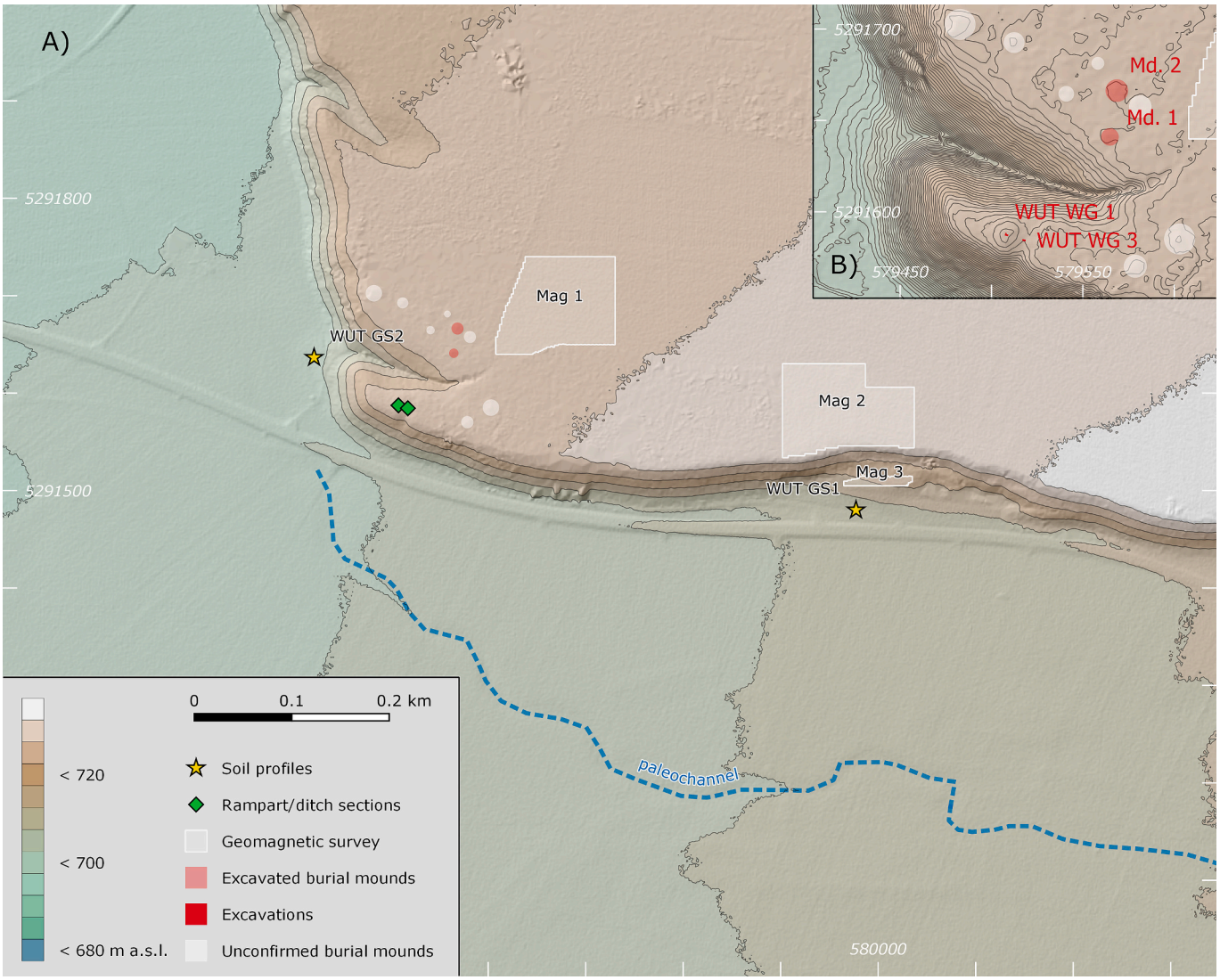


**Fig. 3.** Study site of "Winterstetten Urlauer Tann" (WUT) with the Middle Bronze Age settlement at elevated terrain and colluvial profiles (yellow stars) and with topographic situation. A) shows an overview of the WUT site; B) shows a detailed view of the spur with the rampart-ditch-section (green rhombus), burial mounds (red and white circles) and the conducted geomagnetics (white aea). Coordinates are shown in UTM 32 N reference system; EPSG 25832. Image Credits: LiDAR-DEM (resolution 1 × 1 m, captured in 2002, © LGL Baden-Württemberg, www.lgl-bw.de, Az.: 2851.9–1/19) and official waterway network «AWGN» (© Landesanstalt für Umwelt Baden-Württemberg, downloaded in May 2020 from https://udo.lubw.baden-wuerttemberg.de).

## 3. Material and methods

### 3.1. Field work

Soil scientific and archaeological field work was conducted in 2018 and 2019. Soils were described according to the German guidelines for soil description (Ad-hoc-AG Boden, 2005) and classified according to the World Reference Base for Soil Resources (IUSS Working Group WRB, 2015) by using the translation software of Eberhardt et al. (2014). Soil horizons that were homogeneous, rich in organic matter, in charcoal and sherd fragments and appeared blackish-brown and located along slopes, were labelled as colluvial horizons (M horizons). Along the profiles, M horizons and buried topsoils were sampled in a continuous column with 5 cm depth increments. Different samples were collected for the analysis of charcoal spectra (ca. 1000 g), urease activity and $C_{mic}$ (ca. 100 g), soil micromorphological features and pedogenic and biogeochemical proxies (ca. 300 g, bulk sample). Microbiological samples were cooled during field work and stored at −18 °C. Six samples for micromorphological analysis (10 × 5 cm) were taken in profile WUT GS 1, which referred to MBA colluvial horizons (M3, 99–109 cm; M6, 187–197 cm; M6/M7, 197–207 cm) and the underlying topsoil (2Ahb, 207–217 cm, 2Ahb/2Bwg1, 213–223 cm, 2Bwg1/2Bwg2, 223–233 cm). For luminescence sampling, light-proof steel cylinders were hammered horizontally into the freshly cleaned profiles. Bulk samples were taken around the sample holes of the luminescence cylinders for dose rate determination and water content measurements.

An archaeological excavation was conducted at the LUA site in 2018 and 2019 in collaboration with the State Department for Cultural Heritage, covering an area of ca. 1 ha (Höpfer et al., 2019). A dense series of ca. 1.2 m wide trenches was excavated mechanically by removing the modern topsoil until the undisturbed subsoil was reached. Archaeological features were typically found in the weathered glacial deposits in a depth of ca. 0.5 to 1 m, depending on the palaeorelief. All single features were photographed and mapped digitally, using a Leica TCR 403 Total Station that was set onto a series of reference points which had been measured by dGPS. At the WUT site, field work concentrated on the ditched rampart and on two burial mounds. The former was approached in two small soundings of 2–3 $m^2$, which were excavated horizontally by squares of 0.5 × 0.5 m meters and in 10 cm depth increments. All squares were documented photogrammetrically, giving a georeferenced

photo-mosaic for each planum, as well as the total profiles. Of each burial mound, at least one quarter was excavated. After removing the topsoil, the artificial mound material was excavated by squares of ca. 2 × 2 m in 10 cm depth increments, until the undisturbed subsoil was reached. Single finds were differentiated by squares and spatial measurements were done with the same equipment as at the LUA site. A LTR of Quantum GIS (version 3.10.12 "A Coruña") was used for data processing, evaluation and visualisation. Additionally, a geophysical survey was commissioned from Posselt & Zickgraf Prospektionen GbR. It was conducted in three separate areas on top of the plateau and on a small terrace on its south-facing slope of the WUT site (Fig. 3, Mag. 1, Mag. 2 and Mag. 3), using a Ferex 4.032 DLG Fluxgate-Gradiometer with four CON650-probes (0.65 m distance).

### 3.2. Laboratory analyses

For the analysis of total carbon (TC) and nitrogen (TN), an element analyser ("vario EL III", Elementar Analysesysteme GmbH, Germany, in CNS mode) was used with helium atmosphere and oxidative heat combustion at 1150 °C. Carbonate content ($CaCO_3$) was volumetrically determined using a calcimeter (Eijkelkamp, Giesbeek). Soil organic carbon (SOC) content was determined using the difference of total inorganic carbon (TIC) and TC (Don et al., 2009). Soil pH ($CaCl_2$) was analysed by using a soil:solution ratio of 1:2.5 (Sentix 81, WTW, pH 340). Textural analysis was performed using X-ray granulometry with SediGraph 5120 (Micromeritics GmbH, Germany) for grain sizes <20 µm; grain sizes between 20 and 2000 µm were determined by sieving.

For the soil micromorphological analysis, the oriented samples were impregnated with Viscovoss N50S resin and MEKP505F hardener after air drying. After curing of the resin, the specimens were formatted into blocks (60 × 90 mm) and cut in half (Woco Top 250 A1, Uniprec), ground (encapsulated precision grinding machine LDQ 6100, Huayid), and mounted on a glass. Subsequently, the specimens were cut into approx. 100 µm thick slices and then ground to 30 µm. The thin sections were analysed following the terminology of Stoops (2003) using a polarizing microscope (Zeiss Axio Imager.A2m; Software AxioVision 4.7.2). Fluorescence microscopy was performed using a Colibri.2 system with a multiband passfilter for UV and blue light. Oblique incident light (OIL) was obtained by an external light source with a two-armed gooseneck glass fibre light guide. In addition, the thin sections were scanned at 1200 dpi with a flatbed scanner equipped with transparent light.

Samples for OSL dating were analysed using the coarse grain quartz fraction (90–200 µm). Sample preparation included wet sieving, destruction of calcium carbonates using 10% HCl and organic matter using 10% $H_2O_2$, heavy liquid density separation of the quartz-rich fraction (> 2.63 and < 2.68 g $cm^{-3}$), purification using 40% HF (for 45 min) and rinsing with 10% HCl. The paleodose (De) was determined using a standard SAR protocol following Murray and Wintle (2000, 2003) and performed on Lexsyg luminescence readers (type Smart and Research) using green LED (525 ± 25 mm) stimulation at 70 mW $cm^{-2}$. Signal detection was restricted to ca. 350–400 nm by using the optical filters Semrock HC377/50 filter and SchottBG3 filter. For standard measurement the coarse grain fraction was mounted onto 2 mm stainless steel discs and onto 3 mm discs for test measurements. The latter included a preheat test, analysing natural doses using different preheat temperatures, and a dose recovery test, determining artificial doses combined with varying preheat temperatures. A test on feldspar contamination was conducted at the end of each SAR cycle (Duller, 2003). Radionuclide concentrations were analysed either via a combination of thick source alpha-counting (for U and Th) and ICP-OES (for K), or via a combination of alpha- and beta-counting in the newly developed µdose system (Tudyka et al., 2020).

Charcoal fragments for AMS-$^{14}$C dating were collected from soil profiles and archaeological features and were analysed at the Klaus-Tschira-Lab at the Curt-Engelhorn-Centre of Archaeometry in Mannheim. Samples were pre-treated using the acid-base-acid method (Steinhof et al., 2017). The $^{14}$C ages were normalized to $\delta^{13}C = -25$ ‰ (Stuiver and Polach, 1977). SwissCal 1.0 and the IntCal13 calibration curve (Reimer et al., 2013) were used for calibrating $^{14}$C ages to calendar years.

For the anthracological determination of charcoals, 898 fragments from two colluvial profiles (LKTT 1, WUT GS 1) and 26 fragments from archaeological profiles (WUT WG1, WUT WG3) were retrieved by flotation. The transversal, tangential and radial sections of charcoal were investigated for diagnostic features, using 60× to 500× magnifications. For determination of wood species identification literature (Schweingruber, 1990a, 1990b) was consulted as well as the charcoal reference collection of the Archaeobotany Laboratory at the University of Tübingen. Due to high fragmentation of the charcoal, not all fragments could be identified to the genus level. For example, in some cases it could not be determined whether it was *Quercus* or *Castanea*, or *Populus* or *Salix*; in other cases, it could just be determined whether it was a conifer or dicotyledon.

The extraction of phytoliths (LKTT 1, WUT GS1) followed the procedure outlined by Katz et al. (2010). Approximately 50 mg of sediment was placed into a microcentrifuge tube and 50 µl of 6 M HCl was used to dissolve carbonate components. Phytoliths were isolated according to their density using 450 µl of 2.4 g $l^{-1}$ sodium polytungstate [$Na_6(H_2W_{12}O_{40})*H_2O$] heavy liquid solution. The samples were placed in an ultrasonic bath for 20 min to deflocculate the clays and then centrifuged at 5000 rpm for 5 min. After transferring the supernatant to a clean tube, 50 µl was placed on a microscope slide for phytolith identification and counting. After slide preparation, the number of phytoliths within 16 fields of view were counted and used to extrapolate the concentrations of phytoliths per gram of sediment (Katz et al., 2010). Morphological identification of the phytoliths followed the standard literature (e.g., Piperno, 2006; Twiss et al., 1969) and the International Code for Phytolith Nomenclature (Madella et al., 2005; Neumann et al., 2019). When possible, a minimum of 200 phytoliths were identified on each slide to achieve statistical significance. As many phytoliths as possible were identified in samples that did not meet this threshold, but these were not used for the next level of interpretation based on the plant families and anatomical parts. The phytolith morphotypes were grouped into three main categories, each with more specific subcategories: dicotyledonous plants (leaves/stems, wood/bark); monocotyledonous plants (general, leaves/stems, inflorescences, short cells), and weathered (unidentifiable).

Polycyclic aromatic hydrocarbons (PAHs) were analysed using a modified protocol of Bläsing et al. (2016). A speed extractor (E-916, Büchi Labortechnik GmbH, Germany) was used for extracting 10 g of soil sample (DCM: MeOH, 9:1 *v*/v; method setup: 40 min static time for each run, 2 cycles, 120 °C, 110 bars). Solid Phase Extraction (SPE) was used for sample purification according to Lehndorff and Schwark (2009). The extracts were concentrated and spiked with 10 ng $\mu l^{-1}$ of Pyrene-d10 (internal standard, Sigma Aldrich, Germany). The quantification of PAHs was performed using gas chromatography (GC, Agilent Technologies 7890B, Germany) coupled with mass spectrometry (MS/MS, EVO 3, Chromtech, Germany) in the selected ion monitoring (SIM) mode. 1 µl was injected to an Optima 5MS fused silica capillary column (30 m × 250 µm × 0.25 µm) with splitless injection (liner: Topaz splitless, 4 mm × 6.5 × 78.5, Restek) mode at 250 °C and an inlet flow of 54 ml $min^{-1}$ and 9.4 psi column pressure. Helium (99.999% purity) was used as carrier gas. The oven temperature program was as follows: 80 °C (hold for 2 min) temperature ramp to 250 °C at 10 °C $min^{-1}$ and to 320 °C at 3 °C $min^{-1}$. For qualitative analysis, an external standard mixture of high and low molecular weight components (QTM-PAHmix: Acenaphthene, Acenaphthylene, Anthracene, Benz[*a*]anthracene, Benzo[*b*]fluoranthene, Benzo[*ghi*]perylene, Benzo(*a*)pyrene, 2-Bromonaphthalene, Chrysene, Dibenz[*a,h*]anthracene, Fluoranthene, Fluorene, Indeno[1,2,3-*cd*]pyrene, Naphthalene, Phenanthrene and Pyrene; Sigma-Aldrich, Germany) was used with a concentration of 10 ng $\mu l^{-1}$.

Extracellular urease derived from soil organisms cleaves urea to $NH^{4+}$ and $CO_2$. Its microbial production is favoured in eutrophic soils (e.g., enriched in animal faeces) and urease-organo-mineral complexes are very stable (Skujiòs and McLaren, 1968). Urease activity was determined colorimetrically according to Kandeler and Gerber (1988). 5 g of soil samples were mixed with an aqueous urea solution (0.08 M) and incubated for 2 h at 37 °C. After incubation, 45.5 ml of 1 M KCl/0.01 M HCl were added and mechanically shaken for 30 min. After filtration with cellulose filters, 4.5 ml of distilled $H_2O$, 2.5 ml of mixture solution (in equal parts: 0.3 M NaOH, nitroprussid-salicylate, $H_2O$) and 1 ml of 0.1% dichlorisocyanurate acid were added to 0.5 ml of filtrate. Synergy HTX multi-mode reader (BioTek) was used for colorimetric measurements at 690 nm.

The substrate-induced respiration method (SIR) (Anderson and Domsch, 1978) was performed for the determination of microbial biomass carbon ($C_{mic}$). Samples were analysed using an automated respirometer system based on electrolytic $O_2$ microcompensation (Scheu, 1992). 20 g of soil samples were supplemented with 4 mg glucose $g^{-1}$ dry weight (water content 40–60% of the water holding capacity). Oxygen consumption rates at 22 °C were determined every 15 min. The mean of the eight lowest measurements during the first 11 h after glucose addition was taken as the maximum initial respiratory response (MIRR). $C_{mic}$ (mg $g^{-1}$ dry weight) was calculated as 38 x MIRR (ml $O_2$ $g^{-1}$ $h^{-1}$). The ratio between urease activity and $C_{mic}$ according to Scherer et al. (2021b) was used to differentiate between past and present input of urea. The extracellular urease is very resistant against microbial turnover and weathering, while $C_{mic}$ serves as proxy for current microbial activity. Hence, elevated urease activity/$C_{mic}$ ratios show evidence of ancient soil eutrophication by human and animal faeces.

Faecal biomarkers (sterols, stanols, stanones) were analysed following a modified protocol according to Prost et al. (2017) and Birk et al. (2012). A Speed Extractor (E-916, Büchi Labortechnik GmbH, Germany) was used for extracting 10 g of soil sample (DCM and MeOH (2:1, 1:3, *v*/v); method setup: 40 min static time for each run, 2 cycles, 120 °C, 110 bars). After extraction, 100 µl of d7-cholest-5-en-3ß-ol (5 ng $µl^{-1}$ in MeOH, Avanti Polar Lipids inc.) were added as internal standard (IS1) and concentrated using Büchi Syncore (Büchi, Switzerland). The total lipid extracts (TLE) were silylanized by using 50 µl *N*,*O*-bis(trimethylsilyl)trifluoroacetamide (BSTFA, Sigma Aldrich) and 10 µl DCM: Pyridine (1:1, v/v, Sigma Aldrich) for 1 h at 80 °C. D6-campesterol (100 µl, 10 ng $µl^{-1}$ in MeOH, Avanti Polar Lipids inc.) was used as IS2. Gas chromatography (GC, Agilent Technologies 7890B, Germany) coupled with mass spectrometry (MS/MS, EVO 3, Chromtech, Germany) was used for TLE analysis. 1 µl was injected to an Optima 5MS fused silica capillary column (30 m × 250 µm × 0.25 µm) with splitless pulsed injection (25 psi until 0.5 min, 50 ml $min^{-1}$ at 1 min) mode at 300 °C and an inlet flow of 50 ml $min^{-1}$ and 9.4 psi column pressure. The oven temperature ramp ranged from 60 to 325 °C (for 5 min holding at 60 °C, for 13 min increasing to 140 °C (10 °C $min^{-1}$), for 72 min increasing to 325 °C (3 °C $min^{-1}$), for 15 min holding at 325 °C). The temperature at the transfer line was set to 300 °C, the electron ionisation to 300 eV and the solvent delay to 6 min. Scan mode was used to identify peak identity and retention times (RT). Selected ion monitoring (SIM), including the masses *m/z 124, 129, 145, 215, 229, 231, 255, 257, 316, 329, 343, 355, 367, 368, 370, 382, 383, 386, 396, 398, 445, 457, 458, 459, 472, 473, 484, 486, 465*, was performed for quantification.

For the dissolutions of the heavy metals (As, Cd, Cr, Cu, Hg, Ni, Pb, Zn) a reverse *aqua regia* solution ($HNO_3$ to HCl ratio 1:3, DIN ISO 11466: 1997–06) was pre-treated in a microwave (MLS GmbH, Germany). Heavy metal contents were determined using an ICP-OES (Optima 5300DV, Perkin Elmer Inc.) equipped with a Miramist nebulizer using the element-specific wavelengths according to Nölte (2003).

## 4. Results

### 4.1. Stratigraphy and related soil features

Seven multi-layered alluvial/colluvial profiles were selected for the archaeopedological analyses (Fig. 4, Table 1). At the LUA site the profiles LKNT 2 (Fig. 4, a*) and LKNT 3 (b*) developed from alluvial sediments of the Eschach river. At least five alluvial deposition phases with a thickness of 200 cm were documented for profile LKNT 2 and seven alluvial horizons with a thickness of 168 cm for profile LKNT 3. The alluvial sediments were dominated by clayey loam texture with slightly opposing, alternating silt and sand contents in the corresponding aM horizons. The profile LKTT 1 (c) showed five colluvial horizons (120 cm) that covered a truncated Cambisol from Würmian gravel deposits and glacial till. The sand content decreased with depth at the expense of increasing amounts of silt and clay. For all profiles the pH-values ranged between 5.0 and 6.9 (mean: 6.2, sd: 0.7, n: 22), showing a weak acidic to neutral soil milieu with slightly increasing values at greater soil depth. The SOC contents varied from 0.5 to 3.7% (mean: 1.1, sd: 0.7, n: 22). The C/N values ranged between 7 and 10 (mean: 9, sd: 0.7, n: 22).

At the WUT site, the WUT GS1 (d) profile showed six colluvial horizons with a thickness of 200 cm, which buried a fully preserved Cambisol. The buried topsoil (2Ahb) was rich in charcoal, burned clay and well-preserved MBA sherds. The colluvial sediments were dominated by sandy to clayey loam with only minor changes in grain size distribution with depth. The WUT GS2 (e) was built up from redeposited Riss glacial sediments (M1, M2) covering Würm-age gravel deposits and glacial till (2Bwg, 2Bg). In between, two alluvial horizons (aM3, aM4) were deposited, marking a paleochannel that is still slightly visible in the grassland south of the site (Fig. 3). The profiles WUT WG1 (f) and WUT WG3 (g) were part of the rampart-ditch-structure built on a Riss moraine hill. WUT WG 1 (105 cm in depth) showed a section of the rampart constructed from anthropogenically redeposited soil material overlying a buried topsoil with accumulated charcoal and burnt clay. The WUT WG3 profile documented the ditch with at least four sedimentation phases (100 cm in total thickness) as a result of rampart erosion. These erosion processes favoured the mobilization of sandy material from the rampart into the ditch, revealing a difference in texture between the anthropogenically redeposited sediments and the in-situ soil. For all profiles the pH-values varied from 3.1 to 7.3 (mean: 5.4, sd: 1.2; n: 36) with differences depending on the vegetation cover. A neutral soil milieu was observed for the grassland profiles (WUT GS1, WUT GS2) and the subsoils at the forest sites (WUT WG1, WUT WG2), while for the topsoil horizons at the forest site pH-values <4 were determined. The SOC contents were between 0.1 and 4.4% (mean: 1.1, sd: 1.1, n: 35) with an increase in SOC contents in deeper colluvial horizons and buried topsoils. The C/N ratio ranged between 6 and 23 (mean: 11, sd: 4.4, mean: 35) with clearly wider ratios at the forest site reflecting partially undecomposed SOM.

The profiles LKTT1 and WUT GS1 were chosen for the analyses of archaeobotanical and biogeochemical proxies due to their well-developed chronostratigraphy and phases of colluvial deposition during the MBA.

### 4.2. Chronostratigraphy

The samples showed partially challenging luminescence characteristics, such as feldspar contamination in some aliquots, dim luminescence signals and incomplete bleaching. Aliquots showing feldspar contamination were identified and rejected from the final age calculation. Aliquots not affected by feldspar contamination showed quartz-typical signals with a dominant fast component. The dim signals were compensated by using larger aliquots of 7 mm for the younger samples, which makes identification and estimation of minimum ages difficult due to the signal averaging on large aliquots. Incomplete bleaching was identified for 6 out of 11 samples from the WUT GS1 profile and for 6 out

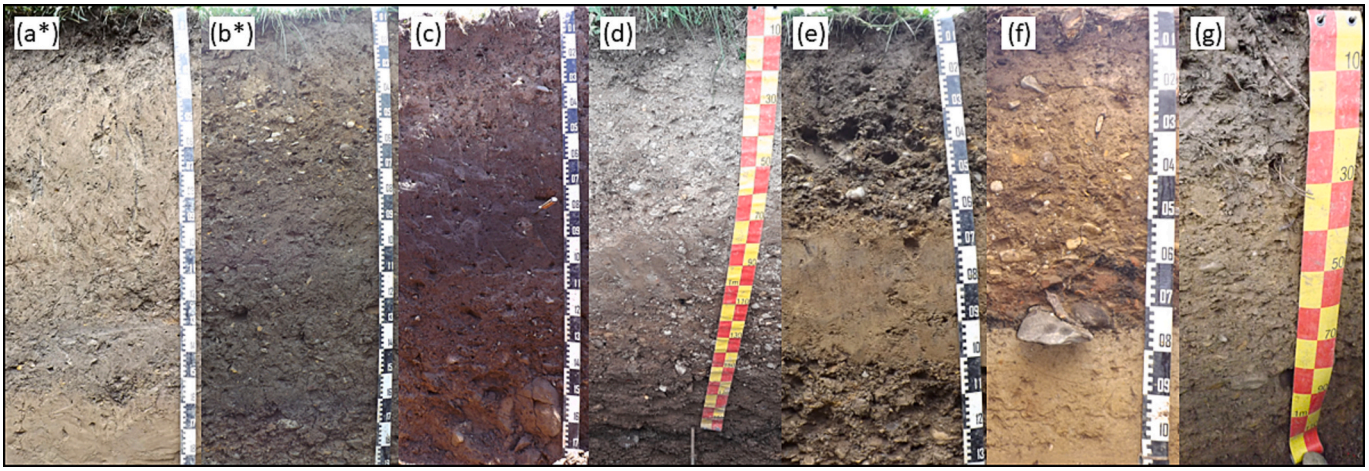


**Fig. 4.** Colluvial/alluvial profiles near Middle Bronze Age settlements. (a*) LKNT 2, (b*) LKNT 3, (c) LKTT 1, (d) WUT GS 1, (e) WUT GS 2, (f) WUT WG 1, (g) WUT WG3, * alluvial. The lower parts of the profiles were cut out due to the depth of the profiles.

of 9 samples from the LKNT 2 and LKTT 1 profiles. These ages were calculated using a bootstrap minimum age model (Galbraith et al., 1999; Cunningham and Wallinga, 2012) with a sigma-b value of 12% (LKNT 2 and LKTT 1) and 13% (WUT GS1). For the well bleached samples, the Central Age Model (Galbraith et al., 1999) was used for the final age calculation. Resulting ages are in correct chronostratigraphic order and are summarised in Fig. 5 and table S1, along with $D_e$ values, the number of accepted aliquots and the underlying age model.

The AMS $^{14}C$ ages showed a correct chronological trend with only few age reversals on a 2-sigma significance level (Fig. 5 and 6, Table S2). From the colluvial soils and the archaeological structures, a total of 62 charcoal fragment were dated of which 32 range into the MBA. OSL and $^{14}C$ ages from the same sampling depth were mostly complementary.

### 4.3. Micromorphology

With the exception of the M3 (99–109 cm) and the 2Ahb/2Bwg2 horizon (223–233 cm) a compacted crumbly to subangular blocky microstructure with high porosity was characteristic in all thin sections of WUT GS1 (Fig. 7, a). Channel microstructure occurred in the M3/M4 transition and compacted granular microstructure in the 2Ahb/2Bwg2 horizon. Features related to layering were not detected. The highest proportion of large charcoal fragments (> 1 mm) was found in the 2Ahb (207–217 cm), slightly less in the overlying M6 horizon (197–207 cm) and the underlying 2Ahb/2Bwg1 horizon (213–223 cm) and sporadically in the M3/M4 and M6 horizons (Fig. 7, c). In these three horizons there was also the highest proportion of coarse material, apart from charcoal fragments consisting of individual mineral grains and rock fragments (mainly chert, siltstones, glauconite-rich sandstones and metamorphic rocks). A bone fragment with a length of 1.6 mm and with an angular shape was found in 2Ahb horizon (Fig. 7, b). The micromass was dominated by stipple speckled b-fabric. Striated, granostriated, porostriated b-fabric occurred only in the 2Ahb/2Bwg1 horizon, in which typical ferruginous nodules and ferruginous hypocoatings on groundmass reflect redoximorphic conditions. Clay coatings could be observed in all horizons. Very dusty blackish clay coatings were present only in M6 (187–197 cm), M6/2Ahb and 2Ahb horizons. Limpid coatings were found only in the buried soil horizons, not in colluvial horizons and brown dusty clay coatings to silt-clay coatings were present only in M6, M6/2Ahb and the 2Ahb/2Bwg2 horizons (Fig. 7, d). Despite frequent passage features and incomplete continuous infillings, indicating reworking by soil mesofauna in all thin sections, no fragments of clay coatings could be detected.

### 4.4. Archaeological records

At the LUA site, both topsoils and archaeological features generally contained few finds. A single, small and unsheltered fireplace was found in the southwest. In addition, few postholes were concentrated in the northwest and southeast of the excavated area. In between, only a scarce scattering of features could be detected. In the southeast, regularly arranged postholes of a northwest-southeast oriented building (Bldg. 1) were identified. They form a rectangular shape about 7.6 m wide and at least 11 m long with symmetrically placed posts. Two charcoal samples taken from the centres of two postholes support a chronological placement in the younger MBA (1400–1300 BCE).

At the WUT site the rampart was built on the fossil topsoil and consists of Riss glacial till and loess derivates containing considerable amounts of stray MBA pottery. Under the western (inner) base of the rampart the edge of a charcoal concentration was found on the fossil topsoil. Its structure and function remained unclear in the small excavation trench, but according to a Pürckhauer prospection, it covers only a few square metres. Therefore, it is probably not indicative of a larger fire event, but rather some small-scale firing site. The good charcoal preservation suggests that it had been quickly covered under the subsequent rampart materials. The ditch had an artificially steepened slope towards the rampart, resulting in a total height of about 3 m (without superstructures). A majority of $^{14}C$ ages from the rampart and ditch layers dates to the EBA (Fig. 6). However, two ages from the firing site provide a solid *terminus post quem* for the rampart erection within or, allowing for old wood effects, shortly after the 16th century BCE, which is also congruent with the pottery. Some of the EBA dates may be explained through old wood effects or can be indicators of genuinely EBA fire events. Several dates from the late 5th and 3rd millennia BCE stem from the fossil top- and subsoils and are not related to the rampart construction. Two much younger dates from the upper rampart layer, however, indicate early medieval activity at the site – whether minor renovation of the rampart, or just superficial activity and subsequent bioturbation. The investigated burial mounds were built from loose soil material, without stone substructions. The original topsoil must have been removed in the intended tumulus' diameter prior to the concentric excavation of subsoil around its later centre, which was then heaped up over the central burial. The smaller mound contained scattered remains of a cremation grave, while the other must have contained a body grave that was later robbed. Both mounds can most likely be dated to the MBA: like the rampart/ditch, their layers contained several EBA charcoals (Fig. 6), but also some stray MBA pottery. Burial mounds like these are uncommon prior to the 16th century BCE in the northwestern Alpine foreland, which is why the EBA dates are explained as fragments of ca. 2

**Table 1**
Soil data of selected profiles. n.a.: not analysed; %: given as mass-%; M: colluvial horizons; aM: alluvial horizons. Values are averaged by horizon.

| Horizon | Depth [cm] | pH [$CaCl_2$] | Clay, silt, sand [%] | SOC [%] | SOC [kg $m^{-2}$] | C/N |
|---|---|---|---|---|---|---|
| | **LKNT 2 (a),** Hypereutric Regosol (Profundihumic, Bathyfluvic) | | | | | |
| Ah | 0–20 | 6.8 | 25,46,29 | 3.7 | 7.2 | 9 |
| aM1 | 20–40 | 6.9 | 29,44,27 | 2.1 | 4.6 | 8 |
| aM2 | 40–96 | 6.7 | 29,42,29 | 0.9 | 6.9 | 8 |
| aM3 | 96–128 | 6.6 | 34,32,34 | 0.8 | 3.3 | 8 |
| aM4 | 128–158 | 6.6 | 35,30,35 | 0.8 | 3.4 | 9 |
| aM-CBg | 158–200 | 6.7 | 31,40,29 | 0.5 | 2.8 | 8 |
| 2CBg | 200–215 | n.a. | n.a. | n.a. | n.a. | n.a. |
| | **LKNT 3 (b),** Hypereutric Regosol (Humic) | | | | | |
| Ah | 0–20 | 5.5 | n.a. | 1.6 | 3.5 | 8 |
| aM1 | 20–36 | 5.7 | n.a. | 1.1 | 1.8 | 8 |
| aM2 | 36–70 | 6.6 | n.a. | 0.7 | 2.5 | 8 |
| aM3 | 70–92 | 6.8 | n.a. | 0.7 | 2.0 | 9 |
| aM4 | 92–111 | 6.7 | n.a. | 0.8 | 2.0 | 10 |
| aM5 | 111–140 | 6.7 | n.a. | 0.9 | 3.0 | 9 |
| aM6 | 140–160 | 6.8 | n.a. | 0.8 | 1.9 | 9 |
| aM-CBg | 160–168 | 6.7 | n.a. | 0.7 | 0.7 | 9 |
| 2CBg | 168–190 | 6.9 | n.a. | 0.5 | n.a. | 7 |
| | **LKTT 1 (c),** Hypereutric Pantocolluvic Regosol (Humic) | | | | | |
| Ah | 0–22 | 5.0 | 16,37,47 | 2.2 | 5.3 | 9 |
| M1 | 22–42 | 5.2 | 24,33,43 | 0.9 | 2.7 | 9 |
| M2 | 42–60 | 5.3 | 24,30,46 | 0.9 | 2.4 | 9 |
| M3 | 60–82 | 5.3 | 24,30,46 | 1.0 | 2.9 | 10 |
| M4 | 82–104 | 5.3 | 20,29,51 | 0.9 | 2.3 | 10 |
| M5 | 104–120 | 5.4 | 20,28,52 | 0.7 | 1.2 | 9 |
| 2Bwg | 120–180 | 5.4 | 20,25,55 | 0.6 | n.a. | 8 |
| | **WUT GS 1 (d),** Hypereutric Anocolluvic Regosol (Humic, Endoraptic) | | | | | |
| Ah | 0–20 | 5.3 | 18,36,46 | 2.9 | 5.4 | 9 |
| M1 | 20–50 | 5.3 | 24,32,44 | 1.2 | n.a. | 10 |
| M2 | 50–75 | 5.5 | 25,30,45 | 0.8 | n.a. | 9 |
| M3 | 75–110 | 5.6 | 27,33,40 | 0.6 | 2.7 | 9 |
| M4 | 110–155 | 5.7 | 28,27,45 | 0.4 | 1.7 | 8 |
| M5 | 155–180 | 5.7 | 27,28,45 | 0.6 | 1.5 | 9 |
| M6 | 180–200 | 5.7 | 25,29,46 | 0.5 | 1.0 | 9 |
| 2Ahb | 200–220 | 5.7 | 26,29,45 | 0.6 | 1.2 | 10 |
| 2Bwg1 | 220–238 | 5.8 | 27,30,43 | 0.4 | 0.5 | 6 |
| 2Bwg2 | 238–260 | 5.9 | 28,37,35 | 0.3 | n.a. | 6 |
| 2CBg1 | 260–265 | 6.0 | 33,40,27 | 0.3 | 1.1 | 6 |
| 2CBg2 | 265–293 | 6.0 | 35,40,25 | 0.3 | 1.1 | 7 |
| | **WUT GS 2 (e),** Endoeutric Dystric Pantocolluvic Regosol (Humic) | | | | | |
| Ah | 0–14 | 4.9 | n.a. | 2.1 | 3.2 | 9 |
| M1 | 14–30 | 5.0 | n.a. | 1.0 | 1.9 | 9 |
| M2 | 30–55 | 5.3 | n.a. | 0.8 | 1.5 | 8 |
| M3 | 55–62 | 5.4 | n.a. | 0.4 | 0.4 | 7 |
| M4 | 62–102 | 5.5 | n.a. | 0.3 | 2.0 | 7 |
| 2Bwg | 102–125 | 6.7 | n.a. | 0.3 | 0.8 | 8 |
| 2Cw | 125–140 | 7.3 | n.a. | 0.1 | 0.2 | <LoD |
| | **WUT WG 1 (f),** Hypereutric Pantocolluvic Regosol (Humic) | | | | | |
| Ah | 0–10 | 3.3 | 22,32,46 | 4.4 | 4.8 | 16 |
| Ah-Bp | 10–15 | 3.6 | 21,38,41 | 3.0 | 1.8 | 15 |
| Bp1 | 15–40 | 3.9 | 25,28,47 | 1.4 | 3.9 | 14 |
| Bp2 | 40–60 | 6.7 | 29,23,48 | 1.1 | 2.6 | 13 |
| Bp3 | 50–70 | 6.9 | 23,29,48 | 1.6 | 3.8 | 16 |
| Ap1 | 64–68 | 6.9 | 19,37,34 | 1.3 | 0.6 | 14 |
| Ap2 | 70–74 | 6.2 | 21,37,42 | 2.2 | 1.1 | 23 |
| Ep | 70–80 | 6.0 | 17,42,41 | 1.5 | 1.8 | 20 |
| 2Bwg1 | 72–89 | 6.6 | 17,45,38 | 0.3 | 0.7 | 10 |
| 2Bwg2 | 89–105 | 6.5 | 18,40,42 | 0.2 | 0.4 | 8 |
| | **WUT WG 3 (g),** Hypereutric Pantocolluvic Regosol (Humic) | | | | | |
| Ah | 0–8 | 3.1 | n.a. | 3.9 | 3.4 | 15 |
| M1 | 8–30 | 3.5 | n.a. | 2.6 | 6.9 | 15 |
| M2 | 30–50 | 3.8 | n.a. | 1.1 | 2.9 | 15 |
| M3 | 50–70 | 3.8 | n.a. | 0.6 | 1.6 | 13 |
| M4 | 70–100 | 4.0 | n.a. | 0.5 | 2.0 | 12 |
| 2Bwg1 | 100–105 | 4.4 | n.a. | 0.4 | 0.3 | 9 |
| 2Bg | 105–115 | 7.1 | n.a. | 0.5 | 0.7 | 11 |

centuries old trees. The magnetograms obtained from the geophysical survey showed no anomalies both on the south facing slope (Mag. 3) and in the eastern plateau above it (Mag. 2). There was a number of promising positive magnetic anomalies in the immediate vicinity of the ditched rampart and the burial mounds (Mag. 1) that very likely indicate archaeological pit features. However, a permission for small scale excavations was not granted by the landowner, so the age and character of these features remain unclear. On the southern slope of the spur, about half a kilometre away from the rampart-ditch-structure, the WUT GS1 profile yielded an amount of charcoal and MBA pottery embedded in the buried topsoil (2Ahb) at a depth of 2 m and covered by six colluvial horizons.

### 4.5. Archaeobotanical proxies

From the charcoal spectra of the LKTT 1 profile, twelve taxa were identified (Fig. 8). The charcoal concentrations were highest in the lower part of M2 (52–60 cm) and the upper part of M3 (60–65 cm). No charcoal of the size 1–2 mm was found in the lower part of 2Bwg (160–180 cm, Fig. 10). In the 2Bwg horizon, *Frangula* was prominently present, while there is only one sample with *Frangula* in a lower depth (75–82 cm, lower part of M3). Other taxa from the 2Bwg horizon were *Betula* and *Acer*, which were not found in the upper part of the profile. From 120 to 125 cm onwards (transition 2Bwg to M5) *Fagus* and *Quercus* were present. *Alnus* and *Populus/Salix* were also present in samples of the M4 and upper part of the M5 horizon. While conifers are not or with a very small proportion (of *Pinus* and *Abies*) represented in the lower part of the profile, from 87 to 92 cm (M4) onwards their proportion increased, and conifers dominated from 70 to 75 cm (M3). They mainly consisted of *Abies* and *Juniperus*. *Quercus/Castanea* remained present throughout the upper horizons of the profile, except for the upper 5 cm of the M1 horizon. *Fagus* concentration decreased with lower profile depth. From the MBA structures of the LUA site, eight charcoal samples were determined and comprised five charcoals from *Abies*, one from *Ulmus*, one from *Juniperus* and one not further identifiable as conifer.

From the charcoal assemblages of the WUT GS1 profile, minimally seven taxa were identified (Fig. 8). In 265–293 cm (2CBg2) and 238–243 cm (2Bwg2) charcoals were unidentifiable due to very small fragment sizes. The highest charcoal concentration was found in the buried topsoil (2Ahb, Fig. 10). Conifers were strongly present throughout the profile, dominated by *Abies* and *Juniperus*. In the lower part of M6 (195–200 cm) another conifer with resin ducts was identified, that may have been either *Larix, Picea* or *Pinus*. *Quercus* was present in the lower part of the profile (2Ahb to 2CBg2), while *Fagus* was present from 205 to 210 cm (2Ahb) onwards. *Hippophaë* was present only in M5 (170–175 cm), just like *Populus/Salix* at 200–205 cm (2Ahb). From the MBA structures at the WUT site, 14 charcoals were determined. In total eight conifers were identified (*Abies*: two, *Juniperus*: six). The remaining samples were identified as *Fagus* (three) and *Fraxinus* (one), while two conifers and one dicotyledon fragment were not further identifiable.

In the LKTT 1 profile the phytoliths were well preserved with high a concentration and 10% or less weathered phytoliths in total (Fig. 10). The concentration tendentially increased with depth with lowest levels in the Ap (~ 2.2 Mio phytoliths per g sediment) and the highest levels in the M5 horizon (~ 3.4 Mio). Remarkably, the upper 5 cm of the M5 horizon showed a lower phytolith concentration compared to under- and overlaying sampling depths. The breakdown into phytolith morphotypes shows no distinct differences throughout the profile with all samples primarily composed of monocotyledonous (monocot) phytoliths (> 80%). Within the monocot phytoliths, the grass short cells (~ 60%) were dominant and leaves/stems (~ 30%), general monocot (~ 6%), and inflorescence phytoliths (~ 2%) in order of decreasing concentration. Only one sample had a small percentage of phytoliths from dicotyledonous (dicot) leaves (~ 8% of the identified dicot phytoliths in the upper part of M4), and the rest originated in dicot wood and bark.

The WUT GS1 profile showed a poor preservation of phytoliths. The

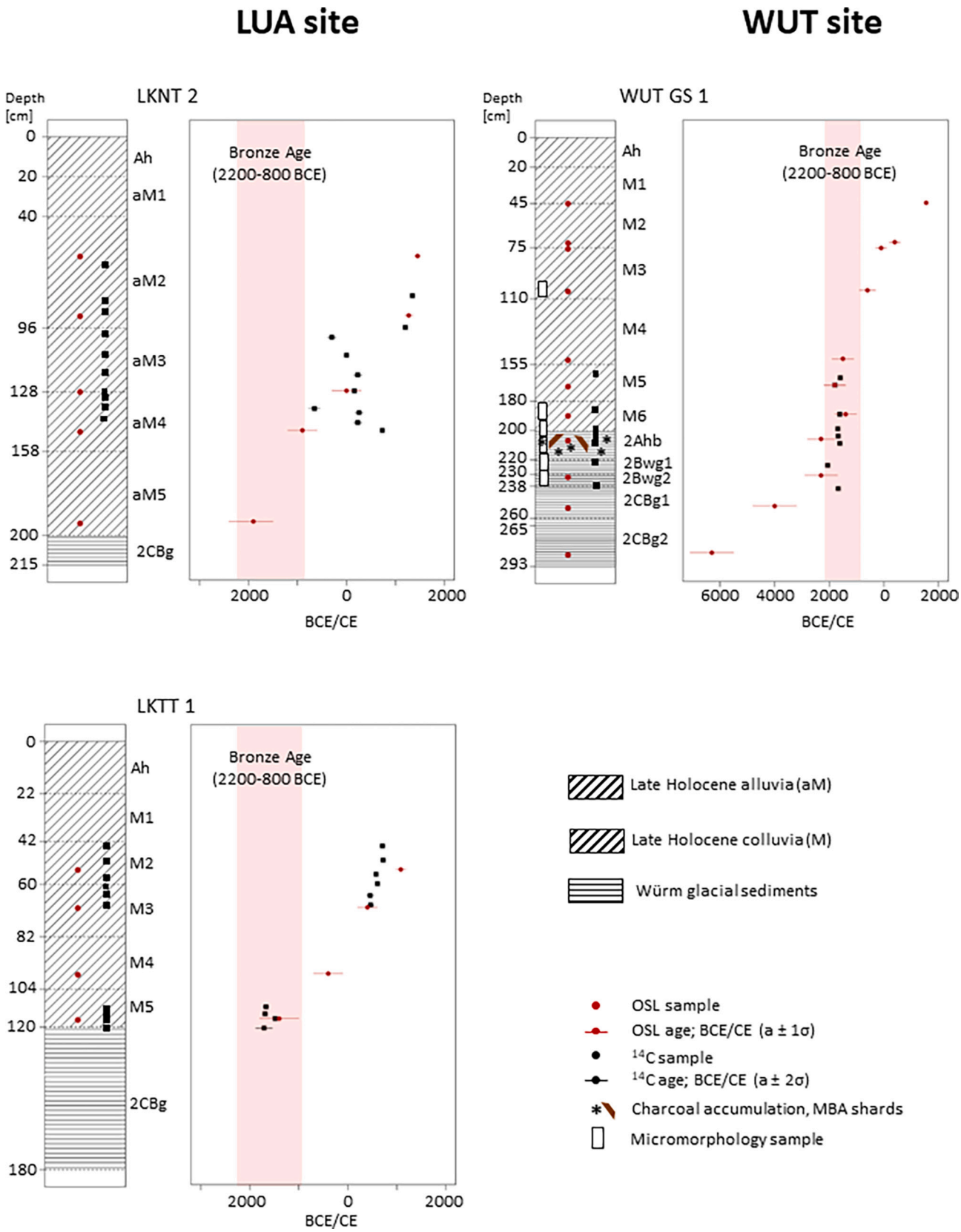


**Fig. 5.** Chronostratigraphy of selected colluvial/alluvial profiles. Colluvial horizons are designated as M, alluvial horizons are designated as aM. BCE: before current era, CE: current era.

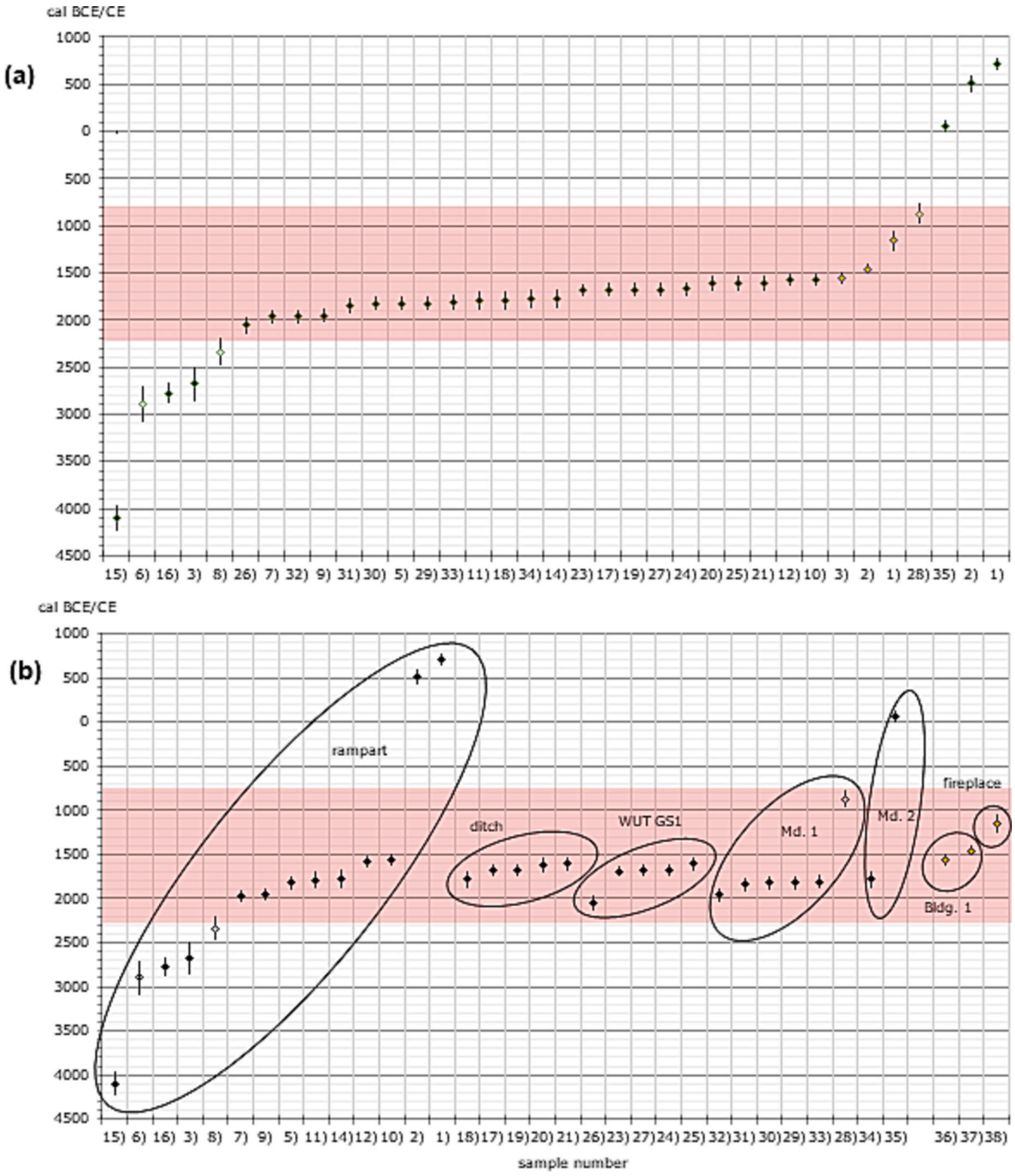


**Fig. 6.** AMS-$^{14}$C ages with 2 sigma error ranges from archaeological features of the LUA and WUT site sorted by (a) chronological order ($^{14}$C ages from the WUT site in black and from the LUA site in yellow rhombi) and (b) archaeological context. Open signatures are dubious samples with low C concentrations. Calibration to calendar years was performed in Oxcal 4.3.2 using IntCal-13 (Reimer et al., 2013); Md. 1: MBA burial mound 1; Md. 2: MBA burial mound 2; Bldg 1: MBA domestic building 1.

highest concentration of ~350,000 phytoliths per g sediment was identified in the Ap horizon, while most of the samples from M3, M4, and M5 have <50,000 phytoliths except for two samples from the upper M3 (75–80 cm, 85–90 cm) and the M4 (120–125 cm) that have >100,000 phytoliths (Fig. 10). There was a distinct increase in the phytolith concentrations from the M6 horizon onwards, with >200,000 phytoliths for M6 and >100,000 for M7. In general, the phytoliths from the WUT GS1 profile were clearly altered, and the assemblage was

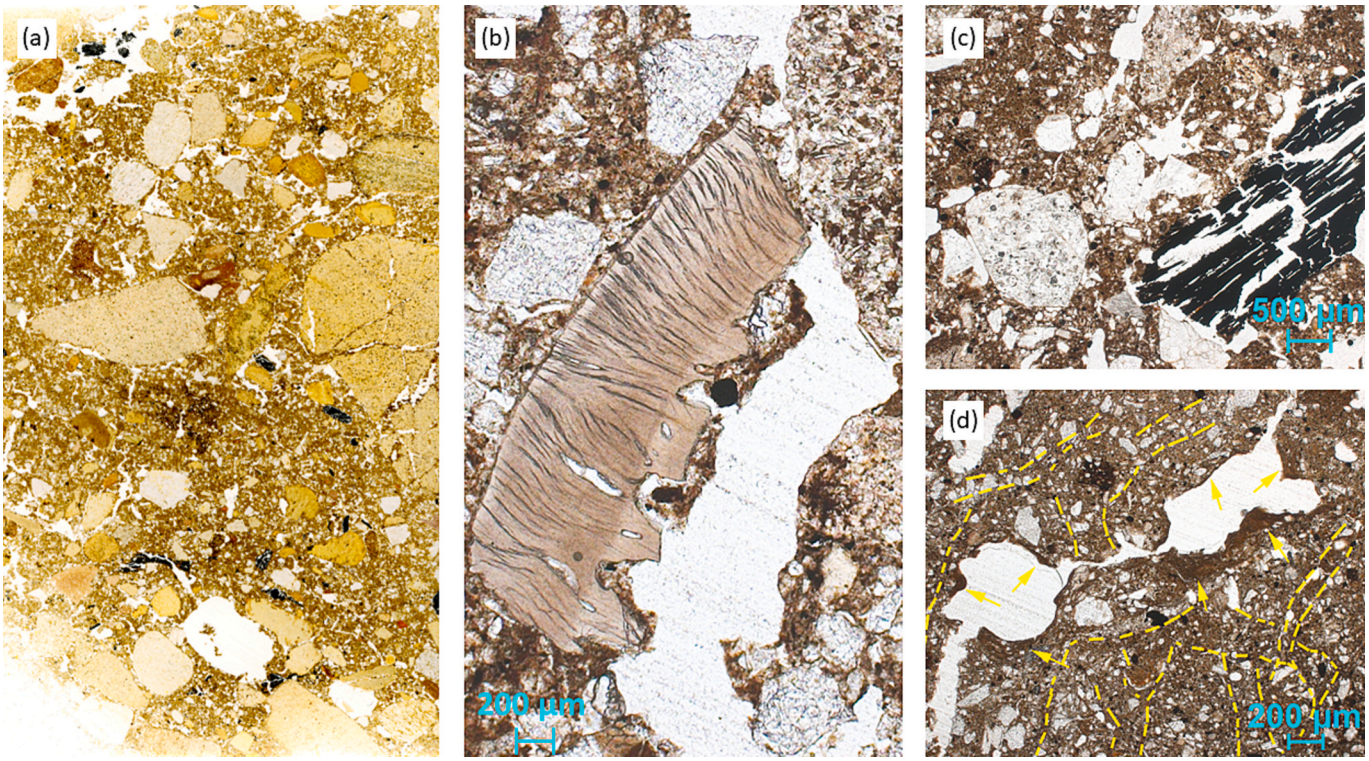


**Fig. 7.** Micromorphological analysis of the profile WUT GS1 (M3/M4, M6, M6/M7, 2Ahb, 2Ahb/2Bwg1, 2Bwg1/2Bwg2). (a) Subangular blocky and compacted granular microstructure. Several charcoal fragments (black areas) –Scan of the thin section 6 × 9 cm – 2 Ahb (207–217 cm); (b) Bone fragment (1.6 mm long) in 2 Ahb (207–217 cm) – ppl.; (c) Large fragment of charcoal (black area) (length > 0.9 mm) in M6 horizon (187–197 cm) – ppl.; (d) Yellow arrows indicate dusty brown clay to silt-clay coatings. Yellow dashed lines comprise passage features – ppl, 2Ahb/2Bwg2 horizon (223–233 cm).

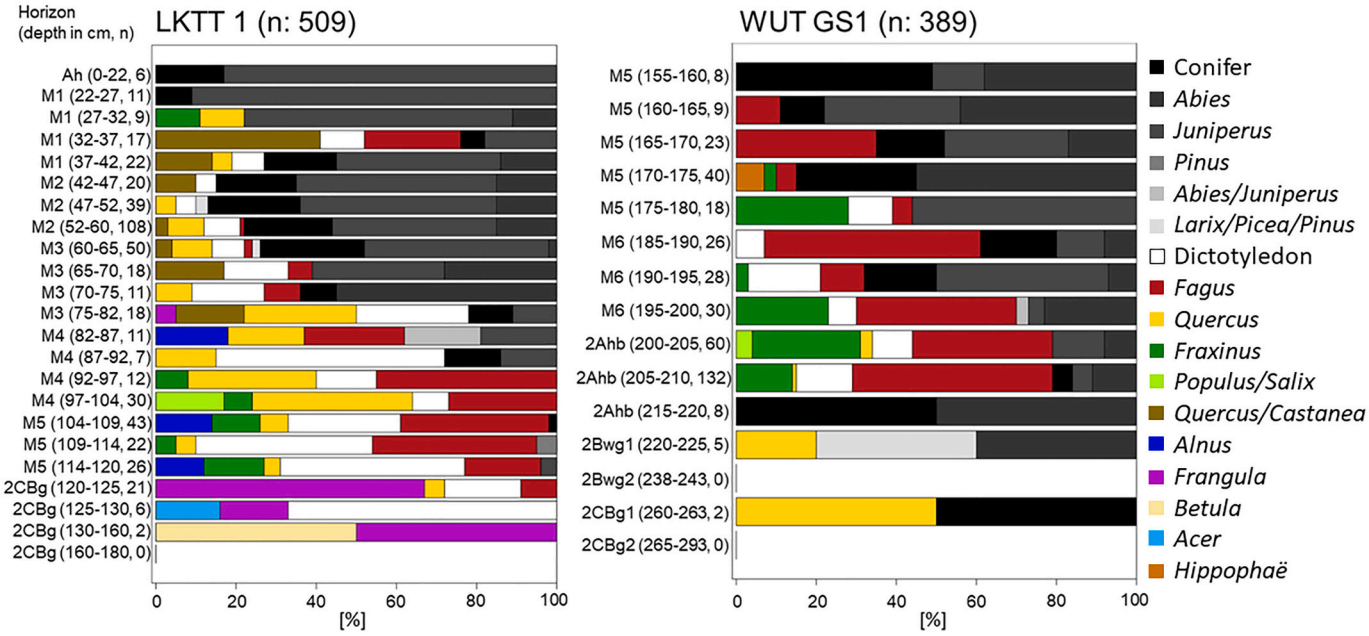


**Fig. 8.** Percentage distribution of charcoal taxa for different sampling depths at the profiles LKTT1 and WUT GS1. n: total number of identified charcoal fragments; Particle size ranges: 1–2 mm, > 2 mm, brackets: horizon designation (sampling depth, number of fragments).

primarily composed of fragments of silica or very weathered phytoliths that could not be attributed to a specific morphotype group. The few identifiable phytoliths were primarily rondel short cells (from Pooid grasses), bulliforms, and prickles (both general monocot phytoliths). These are amongst the most robust types of phytoliths, indicating that there may previously have been more phytoliths present in this profile that were destroyed or dissolved, leaving behind only the resistant types and fragments. However, a weak trend was identified showing a higher

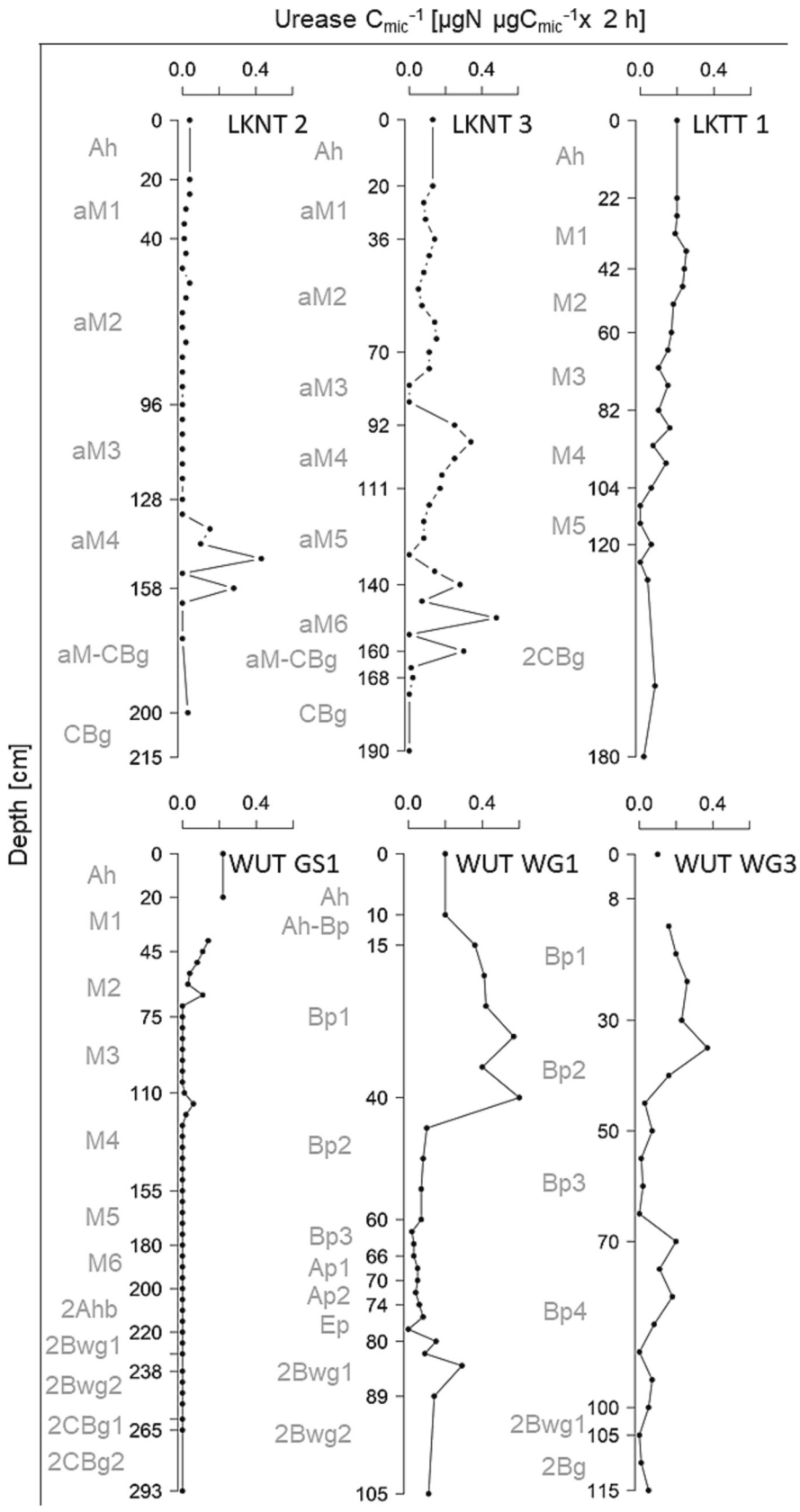


**Fig. 9.** Depth profiles of Urease $C_{mic}^{-1}$ ratio of selected profiles.

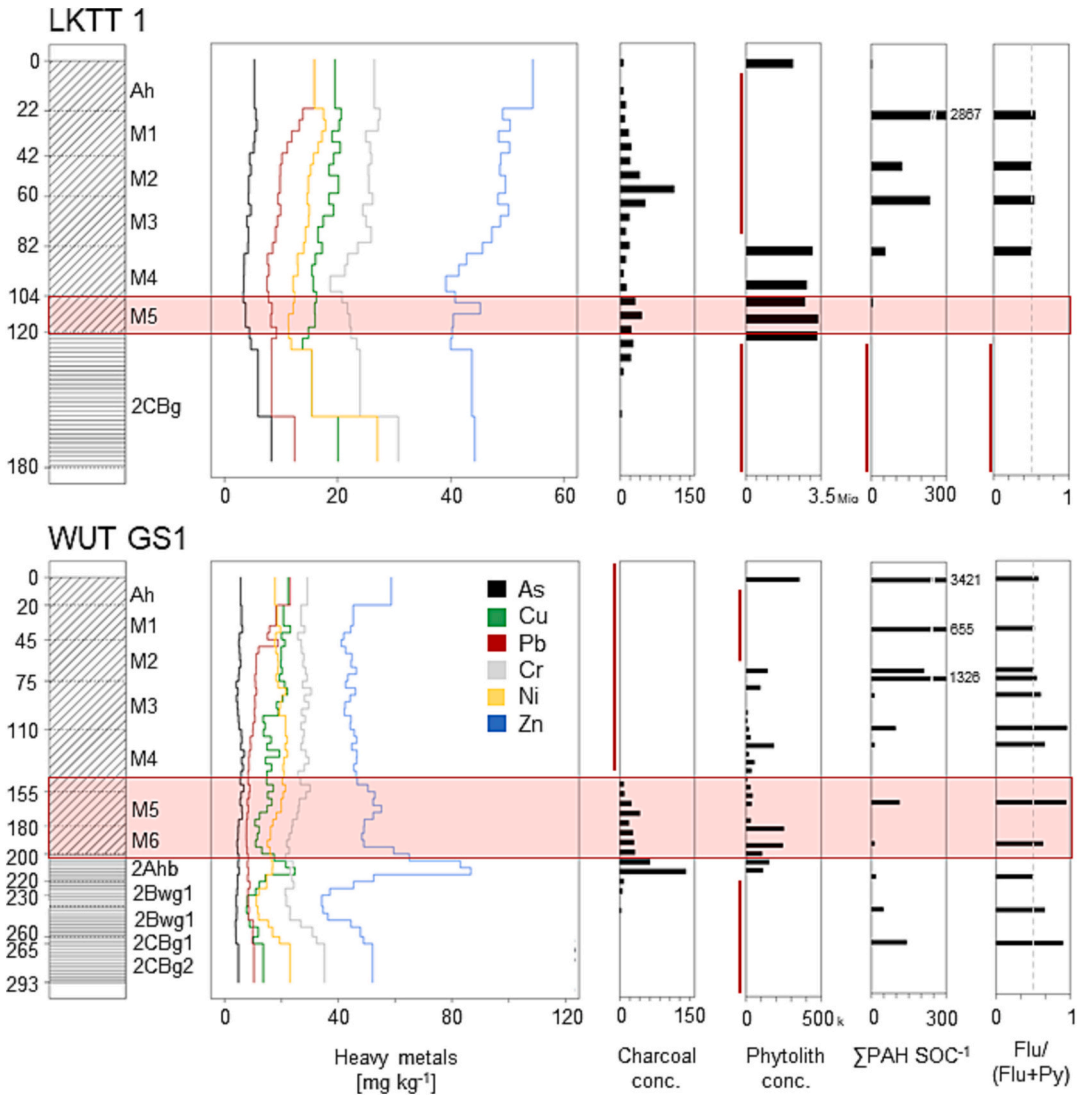


**Fig. 10.** Biogeochemical and archaeobotanical proxies of the profiles LKTT 1 and WUT GS1. As: arsenic, Cr: chrome, Cu: copper, Ni: nickel, Pb: lead, Zn: zinc; ∑PAH/SOC: Ratio of sum of polycyclic aromatic hydrocarbons to soil organic carbon; Flu/(Ful + Py): Ratio of fluoranthene to pyrene with 0.5 threshold as dashed line; red line: depths excluded from analysis.

percentage of dicot phytoliths in the M3 and the upper part of M4 compared to the samples from M6 and M7 samples, which contained only rare dicot and more monocot phytoliths.

### 4.6. Biogeochemical proxies

The heavy metal contents showed a similar trend for all analysed soil profiles (Table S3, Fig. 10): Zn values were highest varying between 21 and 123 mg $kg^{-1}$ (mean: 58, sd: 25, n: 203) and As values were lowest between 3 and 21 mg $kg^{-1}$ (mean: 7, sd: 3, n:203). The range of Pb contents was from 5 to 46 mg $kg^{-1}$ (mean: 14, sd: 7, n: 203), which was below the range of Cr with values from 14 to 89 mg $kg^{-1}$ (mean: 36, sd: 15, n: 203). Cu (mean: 22, sd: 12, n: 203) and Ni contents (mean: 24, sd: 10, sd: 203) were comparable. In all colluvial/alluvial profiles, heavy metal contents were enriched either in the modern topsoil horizons or in the subsoil horizons, which consisted predominantly of poorly weathered parent material. An exception was the WUT GS 1 profile with distinct peaks of Cu and Zn in the 2Ahb horizon. For the profiles of the rampart-ditch-structure, the heavy metal contents were enriched in the horizons consisting of the artificially moved soil material (Bp horizons). Again, Cu and Zn showed additional peaks in the buried topsoil horizon (Ap2). Heavy metals correlated moderately with pH and SOC (Table S5), while for 15% of the correlations $R^2$ were > 0.7. SOC better than pH explained the heavy metal trends.

The urease/$C_{mic}$ ratios were overall low and varied between 0 and 0.6 μg $NH^{4+}$-N $\mu gC_{mic}^{-1} \times 2$ h (Fig. 9, Table S3). The profiles LKTT 1 and WUT GS1 had the highest ratios in the modern topsoil, with no distinct peaks in the underlying colluvial and alluvial horizons. The profiles LKNT 3 and LKNT 2 had peaks of urease/$C_{mic}$ ratios in the deepest alluvial horizons (aM6: 0.48, aM4: 0.43), of which aM4 was dated to the LBA (Urnfield) period (Fig. 5). In the profiles of the rampart-ditch-structure (WUT WG1, WUT WG2), urease/$C_{mic}$ ratios were enriched in the upper horizons up to 40 cm soil depth with a decreasing tendency in the horizons below. For the two colluvial profiles (LKTT1, WUT GS1) there was a weak positive correlation of urease/$C_{mic}$ and SOC as well as urease/$C_{mic}$ and clay ($R^2$: 0.4–0.8, Table S5). There was no correlation between these properties for the alluvial profiles and the profiles from the rampart-ditch-structure.

A total of eleven different PAHs were identified, although not every PAH could be detected in every sample (Table S4). Phenanthrene (Phe) was present in all the samples, while fluorene (Flu) and pyrene (Py) were identified in 89% of the samples. 72% of the samples contained methylated phenanthrenes (M-Phe), while only 39% contained anthracene (Ant) and 28% chrysene (Chy). The single PAH contents were relatively

low (< 1.5 mg $kg^{-1}$ SOC), with Phe, Flu and Py showing the highest levels. From all methylated phenanthrenes, 3 + 2 M-Phe were tendentially higher than 1 + 9 M-Phe. The sum of all PAHs normalized to SOC decreased with increasing soil depth, while peak values could be determined in the modern topsoil and upper colluvial horizons (Ah, M1-M3). In the WUT GS 1 profile, minor peaks of ∑PAH/SOC were detected in the lower part of M5 and 2CBg1 horizon. The Flu to Py ratio indicating the combustion of grass, wood and coal with ratios >0.5 (Yunker et al., 2002), shows no trend with soil depth and has predominantly values between 0.4 and 0.6. Single peaks (> 0.8) were detected in the WUT GS1 profile for horizons M4, M5 and 2CBg1.

With only seven identified steroid compounds, the preservation of faecal biomarker such as stanols and $\Delta^5$ sterols in the WUT GS1 profile is low (< 2 ng $g^{-1}$ SOC). Coprostanol, epicoprostanol and cholestanone were dominant in all horizons (in average > 30% of the total steroid suite). Given the low diversity of stanols and $\Delta^5$ sterols, a diet-specific differentiation between herbivorous and omnivorous lifestyle was not possible by calculating molecular ratios (Leeming et al., 1996). Thus, faecal biomarkers were excluded from further discussion.

## 5. Discussion

### 5.1. Middle Bronze Age subsistence farming in the Western Allgäu

Research on prehistoric subsistence farming mainly focuses on areas favourable for agriculture, since confirmed archaeological finds and favourable environmental conditions suggest widespread land use in the surroundings of prehistoric settlements (Bogaard et al., 2013; Miera, 2020). However, land use activities have also been documented in agriculturally unfavourable areas of southern Germany (Henkner et al., 2018; Kothieringer et al., 2023), leading to the assumption that prehistoric farmers adapted their agricultural techniques to harsher environmental conditions (Teuber et al., 2017). Significant human impact in the Western Allgäu in the shape of agrarian land use is attested not before the pre-Roman Iron Age (Rösch et al., 2020; Tserendorj et al., 2021). Evidence for Bronze Age subsistence farming in the Allgäu region has been derived so far only from off-site pollen spectra without linking them to a specific settlement (Friedmann and Stojakowits, 2017).

#### 5.1.1. Chronostratigraphy of sedimentation phases

The chronostratigraphy of colluvial and alluvial horizons based on OSL and AMS-$^{14}$C dating and its correlation to archaeological structures provide a temporal framework of land use phases (Fuchs and Lang, 2009) and is therefore essential for reconstructing ancient subsistence farming (Dreibrodt et al., 2020; Kittel, 2014; Miera et al., 2019). This reciprocal validation of chronological data yields a robust local chronostratigraphy, even taken into account the larger uncertainties of the numerical dating approaches compared to archaeological definitions.

At the LUA site phases of colluvial deposition during the MBA are shown by OSL dating for the deepest colluvial horizon of the LKTT 1 profile (M5, 1400 ± 300 BCE), located about one km north of the MBA settlement site. Radiocarbon ages of charcoal from the same depth as well as archaeological features such as fireplaces and architectural remains from the excavation area confirm MBA land use activities. The alluvial profile of LKNT 2, which is almost adjacent to the settlement area, shows no depositional phases during the MBA, but during the late EBA (aM5, 1900 ± 400 BCE) and LBA (aM4, 900 ± 300 BCE). This indicates a phase of stability within the alluvial system of the Eschach river during the MBA, either reflecting extensive land use in a sparsely populated landscape or drier and warmer conditions during the MBA compared to previous and subsequent periods (Henkner et al., 2017; Maise, 2022). The LKTT 1 profile, however, points to an onset of agricultural land use, specifically of topsoil erosion due to e.g., ploughing, during the MBA. At the WUT site, an MBA settlement complex consisting of a rampart-ditch-structure and burial mounds on a hilltop, as well as indications of a valley settlement, confirm occupation during the MBA. This occupation is accompanied by the formation of three colluvial horizons (M6 to M4) of profile WUT GS1, which formed simultaneously during the MBA, considering the error range of OSL ages (M6, 1400 ± 400 BCE; M5, 1800 ± 300 BCE; M4, 1500 ± 300 BCE). Thus, up to 90 cm of the soil column was deposited within a few centuries, burying a topsoil with final Neolithic to early EBA ages (2Ahb, 2300 ± 300 BCE). While EBA $^{14}$C ages from this buried topsoil either indicate EBA land use activities before the formation of MBA colluvial horizons or reflect the burning of old trees during the MBA (old wood-effect, Hajdas et al., 2017), the large quantity of MBA domestic pottery found in the buried topsoil (2Ahb) clearly shows that there was MBA activity in the vicinity of profile WUT GS1. The thickness of the MBA colluvial horizons and the coinciding $^{14}$C ages indicate intensive land use during the MBA, despite the steep relief and short slope lengths, which must have involved massive deforestation. As no colluvial horizons from the EBA and earlier periods have been identified, the transition to the MBA period might have marked a change in subsistence practices in this region of the Western Allgäu with moderate and small-scale land use in the EBA and earlier periods and the onset of widespread intensive land use in the MBA.

#### 5.1.2. Vegetation changes and MBA subsistence practices

Assuming that the Neolithic landscape in the Western Allgäu had to cope with only punctual anthropogenic influences, the vegetation pattern at the transition to the Bronze Age must have been patchy with natural beech-fir-forests (Abieti-Fagenion) and island-like land use areas (Friedmann and Stojakowits, 2017). Based on the charcoal records, a similar vegetation pattern is found in MBA related horizons of the WUTGS 1 profile, while the LKTT 1 profile showed a mixed deciduous forest dominated by *Fagus* and *Quercus* and joined by *Fraxinus, Populus/Salix* and *Alnus*. The appearance of *Quercus* could be either natural, as the profile is located in the former floodplain of the Eschach river (Ellenberg and Leuschner, 2010), or anthropogenic indicating a specific land use. The promotion of open, oak-dominated woodlands near Bronze Age settlements for the extraction of timber, fuelwood and litter as well as pasture has also been suggested (Van der Knaap and Van Leeuwen, 2001; Scherer et al., 2021b). In the M4 of LKTT 1 and in the M6 of WUT GS1, there is a transition from deciduous to conifer forest vegetation, as indicated by the increasing abundance of *Abies* and *Juniperus* at the expense of *Quercus* and *Fagus*. Rösch et al. (2020) showed several phases of *Fagus* decline from the pollen profile of Großer Ursee since the Late Neolithic and associated them with phases of land use. Even though prehistoric occupation of the Western Allgäu region seems to be sparse so far, deforestation was indispensable for subsistence farming. Thus, the increasing dominance of fir was likely influenced by the anthropogenic decline of beech, while the changing climatic conditions with decreasing average temperatures additionally favoured the expansion of *Abies* at the expense of *Fagus* during the Subboreal (Beckmann, 2004; Tinner and Lotter, 2006). The increasing abundance of *Juniperus* in MBA (WUTGS 1) and younger colluvial horizons (LKTT 1) suggests open woodlands, since juniper is light-demanding and cannot rejuvenate in closed forests. *Quercus* and *Juniperus* are commonly associated with forest grazing (Conedera et al., 2017; Hejcman et al., 2013; Novák et al., 2012; Scherer et al., 2021a).

In addition to charcoal spectra, phytolith assemblages contribute to deciphering the (grassland) vegetation cover near prehistoric settlements (Meister et al., 2017; Weißkopf et al., 2014). The perseveration of phytoliths is influenced by depositional and post-depositional processes (Cabanes et al., 2009; Madella and Lancelotti, 2012), while high phytolith concentrations in sediments indicate preservation of the former land surface by rapid sedimentation, as weathering processes and microbial activity drive phytolith turnover (Cabanes et al., 2012). In the colluvial soils of the Western Allgäu, phytolith preservation clearly differs between the analysed profiles, leading to the assumption that depositional processes may have primarily caused the state of preservation, since post-depositional processes were similar. The dominance of

monocot phytoliths over dicot species in both profiles indicates an open landscape with permanent grasslands and more sparsely spread forested areas, even considering that monocot plants naturally produce more phytoliths than dicot plants (Piperno, 2006). An ancient farmland near the LUA site in the Eschach plain (profile LKTT 1) is a possible explanation for the low concentration of inflorescence phytoliths together with a higher abundance of phytoliths from leaves and stems (Dietrich et al., 2019; Kirchner et al., 2022; Scherer et al., 2021b). Since inflorescence phytoliths come from the economically valuable part of the plants, farmers may have removed these plant parts by harvesting followed by processing and storage elsewhere. In contrast, a higher abundance of phytoliths from leaves and stems could also be the result of soil conservation practices, as the useless parts of the plant biomass were (i) either left in the fields, (ii) worked back into the soil and contributed to the formation of soil organic carbon, or were (iii) even returned to the fields through manure. Soil fertility preservation techniques have been known as part of farming practices since the Neolithic (Bakels, 1997; Bogaard, 2004). Whether plant components remained intentionally in the fields, or whether harvesting techniques prevented the grain from being cut close to the ground cannot be clearly determined in the Western Allgäu.

The management of the MBA vegetation mosaic with open grassland areas and sparse woodlands was likely associated with the use of fire, since fire practices such as slash-and-burn agriculture have been assumed to be part of prehistoric land use practices since the Neolithic (Kaal and Mailänder, 2019; Rösch et al., 2014). Charcoal and polycyclic aromatic hydrocarbons (PAHs) that accumulates in soils and are preserved in pedosedimentary archives have been widely interpreted as proxy of past human-fire activity (Tan et al., 2020; Whitlock and Larsen, 2001). While charcoal concentrations from colluvial deposits are interpreted as proxy for local fires, PAHs can provide additional information on regional fire events, as the molecules are transported by aerosols and accumulate by dry and wet deposition (Nam et al., 2018). At both study sites, charcoal fluxes confirm MBA human-fire activity in the Western Allgäu. Especially a prominent charcoal peak in the buried topsoil (2Ahb) of profile WUT GS1 indicates a massive fire event that correlates with the beginning of MBA colluvial deposition and can therefore be interpreted as a result of MBA deforestation. A peak of PAH concentration in the M5 of profile WUT GS1 can be related to MBA fire practices, while the overall low PAH concentrations in relevant colluvial horizons contrast with charcoal peaks from the same depth. There are two possible explanations: (i) The production of higher amounts of low molecular weight PAHs (LMWPAH) compared to high molecular weight PAHs (HMWPAH) supports a distribution of burning residues via aerosol transport on a regional scale that might differ from the original fire source (Kappenberg et al., 2019; Lehndorff and Schwark, 2004). (ii) According to a study of Karp et al. (2020) hot fires ($>$ 600 °C), especially when oxygen was limited, lead to lower PAH concentrations in burning residues. Anthropogenic and forest fires (e.g., slash-and-burn agriculture) reveal higher combustion temperatures than natural and grassland fires (Wolf et al., 2013; Wöstehoff et al., 2022). The ratio of Fluoranthene to Pyrene showed values higher than 0.5 in the M6 and M5 of profile WUT GS1, pointing to burning of biomass such as grass and wood. The burning of wood as part of deforestation practices is also indicated by slightly higher 2+3 M-Phe over 1+9 M-Phe values in the lower part of M5 in profile WUT GS1, since 2+3 M-Phe are thermodynamically more stable and are mainly produced at higher combustion temperatures (Budzinski et al., 1993; Wolf et al., 2013). The enrichment of PAHs in the topsoil horizons mirrors a modern contamination of soils via fossil fuel burning (Yunker et al., 2002).

Besides the human-induced changes of vegetation, prehistoric farmers had to cope with soil depletion and to apply manure to maintain the yield capacities of their soils. The management of animal dung can be traced back to the Neolithic, which led to eutrophication within settlements and adjacent areas (Lauer et al., 2014; Nielsen and Kristiansen, 2014). Traces of eutrophication are well reflected by extracellular urease activities (Borisov and Peters, 2017; Chernysheva et al., 2015), as urease is introduced into soils via excretion or stems from the degradation of nucleic acids as part of the soil microbial necromass. At soil depths with lower levels of currently active microorganisms, urease indicates past input of animal dung, either directly from livestock or indirectly from manuring practices (Scherer et al., 2021b). Urease/$C_{mic}$ peaks in the deepest alluvial horizons of LKNT 2 and LKNT 3 can be associated with the nearby MBA settlement activity at the LUA site and makes livestock farming in the former floodplain of the Eschach River plausible. There is no correlation of urease activity and SOC or clay, as given by Taylor et al. (2002), which would explain the urease/$C_{mic}$ depth gradients.

The analysis of the soil micromorphology in the buried surface horizon (WUT GS1, 2Ahb) shows an intensive land use, as indicated by a high number of micro charcoals and one bone fragment. The angular shape of many charcoals and the bone fragment can only be explained by in situ conditions in the buried soil or by a very short transport distance during the formation processes of the colluvial horizons. Micromorphological analysis could not prove indications of ploughing (Lewis, 2012), which either points to the absence of agricultural activity on this slope or to poor preservation of former ploughing activities. In general, there is lack of knowledge about prehistoric fields and buried plough horizons in the northern Alpine foreland (Scherer et al., 2021b), as plough marks are well preserved in sandy soils, but not in the loamy and stone-rich sediments that are widely spread in Central Europe (Macphail et al., 1990; Prøsch-Danielsen, 1993; Thrane, 1989).

Mining ores and the development of metal tools enabled advances in subsistence practices, such as the bronze sickle for harvesting processes (Falkenstein, 2009). The processing of ores is known to result in an enrichment of heavy metal levels in surrounding sediments, exceeding the geogenic background (Kaiser et al., 2021; Henkner et al., 2017). At both study sites, percolation of heavy metals can be mostly neglected because pH values were around 6, leading to a decrease of cationic metal solubility (Young, 2013). Only in the profiles WUT WG1 and WUT WG2 the pH values dropped $<$4, allowing heavy metals to be transported along the soil column. Distinct peaks of zinc and copper in the M5 of LKTT 1 and in the 2Ahb of WUT GS1 could be interpreted as traces of prehistoric metal processing. However, given the higher SOC contents in these horizons, a natural enrichment of heavy metals due to colloidal organo-metalloid complexes seems more likely. Similar observations were made by Würfel et al. (2010), who analysed sediments from a settlement structure to prove mining in the Inner Alps in Austria. From the analysis of the sorption behavior of metal ions on organic surfaces in the soil solution, they concluded that the enrichment of heavy metals was not anthropogenic but natural. Additionally, prehistoric smelting and ore processing would not be associated with increased zinc concentrations in the metal artefacts and adjacent sediments, even when zinc-bearing ores were used. Due to its high volatility, zinc would be emitted into the atmosphere during smelting (Thornton, 2007). Given the absence of archaeological evidence, the heavy metals contents are best explained by modern contamination of the topsoil (e.g., fertilizer) and by the geological background (Martin, 2009), whereas it seems unlikely that substantial quantities of ores have been processed at the study sites. It remains unclear, however, if occasional metal smelting processes – e.g., for casting and/or repairing everyday tools – would necessarily result in a detectable accumulation of heavy metals in the archaeological horizons.

In summary, it can be said that based on the archaeopedological land use proxies combined with the local archaeological record, Middle Bronze Age subsistence farming could be reconstructed for the Western Allgäu. The identification of MBA colluvial horizons indicate land use activities (deforestation, arable and livestock farming) in the vicinity of the excavated settlements. Similar to other areas of the northern Alpine foreland that have been settled since the Neolithic, first phases of colluvial deposition were described for the MBA in the Western Allgäu, which must have been accompanied by an intensification of subsistence

practices (Scherer et al., 2021b). A diversified MBA subsistence in the Western Allgäu included human induced vegetation changes, forest management and silvopastoral practices, as shown by an open landscape (dominance of monocotyledonous phytoliths) and the promotion of open woodland species (*Quercus, Juniperus*). Fire most probably served to initially open the landscape and to maintain open areas for land use (accumulation of charcoal, identification of PAHs). Microbiological analyses point to livestock farming, which – together with the vegetation changes detected – may have played a crucial role in the MBA subsistence farming in the Western Allgäu.

### 5.2. Comparison of subsistence strategies in the northern Alpine foreland during the Middle Bronze Age

Considering the cultural shift in the northern Alpine foreland with widespread land abandonment around the larger pre-Alpine lakes and the expansion into the inland at the transition from the EBA to the MBA, the question arises whether the nature of subsistence farming was affected by this cultural change or whether it was constant in time and merely transferred from the lakes to the inland areas. Pollen profiles from the Allgäu region show phases of landscape opening since the Bronze Age that were associated with a decline of *Fagus* as a result of deforestation and the dominance of grassland species. However, arable farming was subdominant until the Iron Age with a low amount of Cerealia and ruderal species (Friedmann and Stojakowits, 2017; Rösch et al., 2020). This is consistent with the subsistence practices reconstructed from colluvial and alluvial soils at the LUA and WUT site in the Western Allgäu, which include forest management and silvopastoral practices.

In the Hegau region, which is considered more favourable for prehistoric agriculture compared to the Western Allgäu region, onsite and offsite subsistence practices could be reconstructed in greater detail, providing insights into sophisticated subsistence strategies during the MBA. From pollen profiles, colluvial soils and archaeological structures, cereal cropping is indicated by the dominance of monocotyledon phytoliths, the appearance of cereal species and plough marks. The evidence of five staple crops (*Hordeum distichon/vulgare, Triticum dicoccum, Triticum monococcum, Triticum spelta, Triticum aestivum/turgidum*) typical for the MBA period, along with archaeological evidence for storage facilities (stilted pantries), indicate a sophisticated cropping system with varying sowing and harvesting times, surplus cereal production and fallow land. Livestock farming on fallow land was either part of the cultivation process or a component of coppice management in open, oak-dominated woodlands (Höpfer et al., 2021; Rösch et al., 2014; Scherer et al., 2021b; Tserendorj et al., 2021).

Even though the sedimentary archives of Leutkirch (Western Allgäu) do not allow such detailed insights into MBA subsistence compared to other region of the northern Alpine foreland, our results indicate a diversified land use strategy during the MBA in a supposedly unfavourable landscape. This land use strategy comprises, on the one hand, elements of subsistence already established during the EBA (e.g., Lake Constance, see Rösch et al., 2014) and, on the other hand, MBA subsistence elements from agriculturally favourable areas (e.g., Hegau, see Scherer et al., 2021b). Subsistence farming in agriculturally unfavourable areas was surely accompanied by a certain adaption to harsher climate conditions with crop yields being less predictable and growing seasons shorter. However, the adaption of subsistence strategies to a different landscape could also be associated with the gain of new techniques and the re-evaluations of given environmental resources. One line of thought concerning the Western Allgäu could emphasize the role of the valleys of the Rhenish and Danubian river systems, which were already preferred trading routes transporting tangible resources such as ores and amber in the MBA (Kaul, 2018; Varberg et al., 2020). These trading routes could have played a decisive role in the re-evaluation of a landscape considered unfavourable for agriculture and thus for its colonisation (Mainberger, 2020).

## 6. Conclusion

Archaeopedological investigations of colluvial and alluvial deposits in the immediate vicinity of Middle Bronze Age settlements in the agriculturally unfavourable Western Allgäu region revealed human induced vegetation changes and subsistence practices, especially silvopastoral agriculture, in correlation with the local archaeological records. These subsistence practices were responsible for the formation of a cultural landscape and for colluvial deposition in the Western Allgäu since the Middle Bronze Age. With regard to our hypotheses, we conclude (i) an increasing density of perennial settlements in the Western Allgäu region in the Middle Bronze Age. This pattern is consistent with the general spread of settlements at the transition from the Early to the Middle Bronze Age in the northern Alpine foreland with an abandonment of the pile-dwelling settlements and the occupation of inland areas. From the comparison of the Middle Bronze Age subsistence practices reconstructed from sedimentary archives in the Western Allgäu with subsistence strategies derived from archives on a regional scale, we conclude (ii) a spatial and temporal continuation of subsistence farming in the northern Alpine foreland. We assume that subsistence strategies of MBA farmers were already sophisticated and could be transferred and adapted to different landscape units over time. In addition, the occupation of the previously considered unfavourable Western Allgäu could also be favoured by the re-evaluation of given environmental resources in a landscape. For the Western Allgäu, we conclude that the infrastructure of existing trading routes played a decisive role in valorisation and colonisation of a landscape, which was in large parts unfavourable for agriculture.

Supplementary data to this article can be found online at https://doi.org/10.1016/j.geodrs.2023.e00715.

## Declaration of Competing Interest

The authors declare that they have no known competing financial interests or personal relationships that could have appeared to influence the work reported in this paper.

## Data availability

Data will be made available on request.

## Acknowledgements

This study is part of the Collaborative Research Center 1070 ResourceCultures (SFB 1070) at the Eberhard Karls University Tübingen financed by the German Research Foundation (DFG). We are grateful to many technical assistants and student helpers from the University of Tübingen and the University of Bayreuth who supported the fieldwork and laboratory work, namely Rita Mögenburg, Karin Söllner, Andrey Rodionov and Astrid Paul. We thank the State Department for Cultural Heritage in Baden-Württemberg, represented namely by Prof. Dirk Krausse, Dr. Doris Schmid and Dr. André Spatzier, for providing us with any required information, for supporting us with both advice and equipment, and for permitting all our field work. We are especially grateful to many land owners in the Western Allgäu for allowing us to work on their land.

## References

Ad-hoc-AG Boden der Staatlichen Geologischen Dienste und der Bundesanstalt für Geowissenschaften und Rohstoffe, 2005. Bodenkundliche Kartieranleitung (KA 5), mit 103 Tabellen und 31 Listen. Schweizerbart.

Anderson, J.P.E., Domsch, K.H., 1978. A physiological method for the quantitative measurement of microbial biomass in soils. Soil Biol. Biochem. 10, 215–221. https://doi.org/10.1016/0038-0717(78)90099-8.

Bakels, C.C., 1997. The beginnings of manuring in western Europe. Antiquity 71 (272), 442–445. https://doi.org/10.1017/S0003598X00085057.

Beckmann, M., 2004. Pollenanalytische Untersuchungen der Zeit der Jäger und Sammler und der ersten Bauern an zwei Lokalitäten des Zentralen Schweizer Mittellandes: Umwelt und erste Eingriffe des Menschen in die Vegetation vom Paläolithikum bis zum Jungneolithikum. Dissertationes Botanicae, 390, pp. 1–223.

Birk, J.J., Dippold, M., Wiesenberg, G.L., Glaser, B., 2012. Combined quantification of faecal sterols, stanols, stanones and bile acids in soils and terrestrial sediments by gas chromatography–mass spectrometry. J. Chromatogr. A 1242, 1–10. https://doi.org/10.1016/j.chroma.2012.04.027.

Bläsing, M., Kistler, M., Lehndorff, E., 2016. Emission fingerprint of inland navigation vessels compared with road traffic, domestic heating and ocean going vessels. Org. Geochem. 99, 1–9. https://doi.org/10.1016/j.orggeochem.2016.05.009.

Bogaard, A., 2004. The nature of early farming in central and south-East Europe. Documenta Praehistorica 31, 49–58. https://doi.org/10.4312/dp.31.4.

Bogaard, A., Fraser, R., Heaton, T.H., Wallace, M., Vaiglova, P., Charles, M., Jones, G., Evershed, R.P., Styring, A.K., Andersen, N.H., Arbogast, R.-M., Bartosiewicz, L., Gardeisen, A., Kanstrup, M., Maier, U., Marinova, E., Ninov, L., Schäfer, M., Stephan, E., 2013. Crop manuring and intensive land management by Europe's first farmers. P Natl. A Sci. 110 (31), 12589–12594. https://doi.org/10.1073/pnas.1305918110.

Borisov, A.V., Peters, S., 2017. Geoarchäologische Untersuchungen in Karbadinka 2 und 3. In: Reinhold, S., Korobov, D.A., Belinksij, A.B. (Eds.), Landschaftsarchäologie im Nordkaukasus, Archäologie in Eurasien, pp. 71–94.

Budzinski, H., Garrigues, P., Radke, M., Connan, J., Oudin, J.L., 1993. Thermodynamic calculations on alkylated phenanthrenes: geochemical applications to maturity and origin of hydrocarbons. Org. Geochem. 20 (7), 917–926. https://doi.org/10.1016/0146-6380(93)90103-I.

Cabanes, D., Burjachs, F., Expósito, I., Rodríguez, A., Allué, E., Euba, I., Vergés, J.M., 2009. Formation processes through archaeobotanical remains: the case of the Bronze Age levels in El Mirador cave, Sierra de Atapuerca, Spain. Quat. Int. 193 (1–2), 160–173. https://doi.org/10.1016/j.quaint.2007.08.002.

Cabanes, D., Gadot, Y., Cabanes, M., Finkelstein, I., Weiner, S., Shahack-Gross, R., 2012. Human impact around settlement sites: a phytolith and mineralogical study for assessing site boundaries, phytolith preservation, and implications for spatial reconstructions using plant remains. J. Archeol. Sci. 39 (8), 2697–2705. https://doi.org/10.1016/j.jas.2012.04.008.

Chernysheva, E.V., Korobov, D.S., Khomutova, T.E., Borisov, A.V., 2015. Urease activity in cultural layers at archaeological sites. J. Archaeol. Sci. 57, 24–31. https://doi.org/10.1016/j.jas.2015.01.022.

Conedera, M., Colombaroli, D., Tinner, W., Krebs, P., Whitlock, C., 2017. Insights about past forest dynamics as a tool for present and future forest management in Switzerland. For. Ecol. Manag. 388, 100–112. https://doi.org/10.1016/j.foreco.2016.10.027.

Cunningham, A., Wallinga, J., 2012. Realizing the potential of fluvial archives using robust OSL chronologies. Quat. Geochronol. 12, 98–106. https://doi.org/10.1016/j.quageo.2012.05.007.

Dietrich, L., Meister, J., Dietrich, O., Notroff, J., Kiep, J., Heeb, J., Beuger, A., Schütt, B., 2019. Cereal processing at early Neolithic Göbekli Tepe, southeastern Turkey. PLoS One 14 (5), e0215214. https://doi.org/10.1371/journal.pone.0215214.

Don, A., Scholten, T., Schulze, E.D., 2009. Conversion of cropland into grassland: implications for soil organic-carbon stocks in two soils with different texture. J. Plant Nutr. Soil Sc. 172, 53–62. https://doi.org/10.1002/jpln.200700158.

Dreibrodt, S., Hofmann, R., Sipos, G., Schwark, L., Videiko, M., Shatilo, L., Martini, S., Saggau, P., Bork, H.-R., Kirleis, W., Duttmann, R., Müller, J., 2020. Holocene soil erosion in Eastern Europe-land use and/or climate controlled? The example of a catchment at the Giant Chalcolithic settlement at Maidanetske, Central Ukraine. Geomorphology 367, 107302. https://doi.org/10.1016/j.geomorph.2020.107302.

Duller, G.A.T., 2003. Distinguishing quartz and feldspar in single grain luminescence measurements. Radiat. Meas. 37, 161–165. https://doi.org/10.1016/S1350-4487(02)00170-1.

Eberhardt, E., Schad, P., Berner, T., Lehmann, C., Walthert, L., Pietsch, D., 2014. Ableitungsschlüssel KA5 (2005) nach WRB (2007). Bundesanstalt für Geowissenschaften und Rohstoffe (BGR), Hannover, Germany.

Ellenberg, H., Leuschner, C., 2010. Vegetation Mitteleuropas mit den Alpen: in ökologischer, dynamischer und historischer Sicht, 1095, UTB.

Falkenstein, F., 2009. Zur Subsistenzwirtschaft der Bronzezeit in Mittel-und Südosteuropa. *M. Bartelheim/H. Stäuble (Hg.), Die wirtschaftlichen Grundlagen der Bronzezeit Europas*. Forschungen zur Archäometrie und Altertumswissenschaft 4 (2009), 147–176.

Friedmann, A., Stojakowits, P., 2017. Zur spät- und postglazialen Vegetationsgeschichte des Allgäu mit Alpenanteil. OPUS publications University of Augsburg. https://opus.bibliothek.uni-augsburg.de/opus4/66786.

Fuchs, M., Lang, A., 2009. Luminescence dating of hillslope deposits—a review. Geomorphology 109 (1–2), 17–26. https://doi.org/10.1016/j.geomorph.2008.08.025.

Galbraith, R.F., Roberts, R.G., Laslett, G.M., Yoshida, H., Olley, J.M., 1999. Optical dating of single and multiple grains of quartz from Jinmium rock shelter, northern Australia: part I, experimental design and statistical models. Archaeometry 41, 339–364. https://doi.org/10.1111/j.1475-4754.1999.tb00987.x.

Geyer, O.F., Gwinner, M.P., Geyer, M., Nitsch, E., Simon, T., 2011. Geologie von Baden-Württemberg 5, 627, Schweizerbart Germany.

Hajdas, I., Hendriks, L., Fontana, A., Monegato, G., 2017. Evaluation of preparation methods in radiocarbon dating of old wood. Radiocarbon 59 (3), 727–737. https://doi.org/10.1017/RDC.2016.98.

Harding, A.F., 2000. European Societies in the Bronze Age. Camb. Univ. Press.

Hejcman, M., Hejcmanova, P., Pavlů, V., Beneš, J., 2013. Origin and history of grasslands in Central Europe–a review. Grass Forage Sci. 68 (3), 345–363. https://doi.org/10.1111/gfs.12066.

Henkner, J., Ahlrichs, J.J., Downey, S., Fuchs, M., James, B.R., Knopf, T., Scholten, T., Teuber, S., Kühn, P., 2017. Archaeopedology and chronostratigraphy of colluvial deposits as a proxy for regional land use history (Baar, Southwest Germany). Catena 155, 93–113. https://doi.org/10.1016/j.catena.2017.03.005.

Henkner, J., Ahlrichs, J., Downey, S., Fuchs, M., James, B., Junge, A., Knopf, T., Scholten, T., Kühn, P., 2018. Archaeopedological analysis of colluvial deposits in favourable and unfavourable areas: reconstruction of land use dynamics in SW Germany. R. Soc. Open Sci. 5 (5), 171624. https://doi.org/10.1098/rsos.171624.

Höpfer, B., 2020. Bronzezeitliche Landnutzungsdynamiken und das Siedlungsgefüge der mittleren Bronzezeit im nord-westlichen Alpenvorland. Regionale Entwicklungslinien im Hegau (Lkr. Konstanz) und Westallgäu (Lkr. Ravensburg) mit Fallbeispielen aus Engen-Anselfingen und Leutkirch im Allgäu. Univ. Diss., Tübingen.

Höpfer, B., Rottler, S., Vogt, R., Knopf, T., 2016. Bronzezeit im Hinterland des Bodensees: Siedlungsreste und Kolluvien aus Bodman. In: Fundberichte aus Baden-Württemberg, pp. 53–76.

Höpfer, B., Scherer, S., Schmid, D., Herrmann, J., Scholten, T., Kühn, P., Knopf, T., 2019. Archäologische und bodenkundliche Untersuchungen zur bronzezeitlichen Besiedlung des westlichen Allgäus bei Leutkirch. In: Archäologische Ausgrabungen in Baden-Württemberg 2018, pp. 31–35.

Höpfer, B., Werner, S., Scherer, S., Schmid, D., Scholten, T., Kühn, P., Knopf, T., 2020. Talsiedlung - Höhensiedlung - Bestattungsplatz? Weitere Forschungen zur bronzezeitlichen Besiedlung des Westallgäus bei Leutkirch. In: Archäologische Ausgrabungen in Baden-Württemberg 2019, pp. 24–27.

Höpfer, B., Lutz, J., Krutter, S., Scherer, S., Kühn, P., Scholten, T., Knopf, T., 2021. Mitterbergkupfer am Bodensee? Ein Gusskuchenfragment aus der mittelbronzezeitlichen Siedlung von Engen-Anselfingen (Lkr. Konstanz, Baden-Württemberg). Archäologisches Korrespondenzblatt 51 (4), 501–516. https://doi.org/10.11588/ak.2021.4.93267.

IUSS Working Group WRB: World reference base for soil resources 2014, 2015. update International soil classification system for naming soils and creating legends for soil maps. World soil resources reports No. 106. http://www.fao.org/3/a-i3794en.pdf.

James, B.R., Teuber, S., Miera, J.J., Downey, S., Henkner, J., Knopf, T., Correa, F.A., Höpfer, B., Scherer, S., Michaelis, A., Wessel, B.M., Gibbons, K.S., Kühn, P., Scholten, T., 2021. Soils, landscapes, and cultural concepts of favor and disfavor within complex adaptive systems and ResourceCultures: human-land interactions during the Holocene. Ecol. Soc. 26, 1. https://doi.org/10.5751/ES-12155-260106.

Jansen, B., Wiesenberg, G.L.B., 2017. Opportunities and limitations related to the application of plant-derived lipid molecular proxies in soil science. SOIL 3, 211–234. https://doi.org/10.5194/soil-3-211-2017.

Kaal, J., Mailänder, S., 2019. Molecular properties of soil organic matter in dark buried colluvium from South Germany show abundance of fire residues from Early Neolithic vegetation clearance and slash and burn agriculture. In: Analytical Pyrolysis Letters, APL004, pp. 1–10.

Kaiser, K., Tolksdorf, J.F., de Boer, A.M., Herbig, C., Hieke, F., Kasprzak, M., Kočár, P., Petr, L., Schubert, M., Schröder, F., Fülling, A., Hemker, C., 2021. Colluvial sediments originating from past land-use activities in the Erzgebirge Mountains, Central Europe: occurrence, properties, and historic environmental implications. Archaeol. Anthropol. Sci. 13, 1–26. https://doi.org/10.1007/s12520-021-01469-z.

Kandeler, E., Gerber, H., 1988. Short-term assay of soil urease activity using colorimetric determination of ammonium. Biol. Fertil. Soils 6, 68–72. https://doi.org/10.1007/BF00257924.

Kappenberg, A., Braun, M., Amelung, W., Lehndorff, E., 2019. Fire condensates and charcoals: chemical composition and fuel source identification. Org. Geochem. 130, 43–50. https://doi.org/10.1016/j.orggeochem.2019.01.009.

Karp, A.T., Holman, A.I., Hopper, P., Grice, K., Freeman, K.H., 2020. Fire distinguishers: refined interpretations of polycyclic aromatic hydrocarbons for paleo-applications. Geochim. Cosmochim. Acta 289, 93–113. https://doi.org/10.1016/j.gca.2020.08.024.

Katz, O., Cabanes, D., Weiner, S., Maeir, A.M., Boaretto, E., Shahack-Gross, R., 2010. Rapid phytolith extraction for analysis of phytolith concentrations and assemblages during an excavation: an application at Tell es-Safi/Gath, Israel. J. Archaeol. Sci. 37, 1557–1563. https://doi.org/10.1016/j.jas.2010.01.016.

Kaul, F., 2018. Middle Bronze Age long distance exchange: early glass, amber and guest-friendship, Xenia. In: Bronzezeitlicher Transport. Akteure, Mittel und Wege, 189-211, RessourcenKulturen 8. Tübingen University Press.

Kirchner, A., Herrmann, N., Matras, P., Müller, I., Meister, J., Schattner, T.G., 2022. A pedo-geomorphological view on land use and its potential in the surroundings of the ancient Hispano-Roman city Munigua (Seville, SW Spain). E&G Quat. Sci. J 71, 123–143. https://doi.org/10.5194/egqsj-71-123-2022.

Kittel, P., 2014. Slope deposits as an indicator of anthropopressure in the light of research in Central Poland. Quat. Int. 324, 34–55. https://doi.org/10.1016/j.quaint.2013.07.021.

Kothieringer, K., Seregély, T., Jansen, D., Steup, R., Schäfer, A., Lambers, K., Fuchs, M., 2023. Mid-to Late Holocene landscape dynamics and rural settlement in the uplands of northern Bavaria, Germany. Geoarchaeology 38 (2), 220–245. https://doi.org/10.1002/gea.21952.

Kühn, P., Lehndorff, E., Fuchs, M., 2017. Lateglacial to Holocene pedogenesis and formation of colluvial deposits in a loess landscape of Central Europe (Wetterau, Germany). Catena 154, 118–135. https://doi.org/10.1016/j.catena.2017.02.015.

Lauer, F., Prost, K., Gerlach, R., Paetzold, S., Wolf, M., Urmersbach, S., Lehndorff, E., Eckmeier, E., Amelung, W., 2014. Organic fertilization and sufficient nutrient status in prehistoric agriculture? - indications from multi-proxy analyses of archaeological

topsoil relicts. PLoS One 9 (9), e106244. https://doi.org/10.1371/journal.pone.0106244.
Leeming, R., Ball, A., Ashbolt, N., Nichols, P., 1996. Using faecal sterols from humans and animals to distinguish faecal pollution in receiving waters. Water Res. 30, 2893–2900. https://doi.org/10.1016/S0043-1354(96)00011-5.
Lehndorff, E., Schwark, L., 2004. Biomonitoring of air quality in the Cologne Conurbation using pine needles as a passive sampler – part II: polycyclic aromatic hydrocarbons (PAH). Atmos. Environ. 38, 3793–3808. https://doi.org/10.1016/j.atmosenv.2004.03.065.
Lehndorff, E., Schwark, L., 2009. Biomonitoring airborne parent and alkylated three-ring PAHs in the greater Cologne Conurbation I: temporal accumulation patterns. Environ. Pollut. 157, 1323–1331. https://doi.org/10.1016/j.envpol.2008.11.037.
Lewis, H., 2012. Investigating Ancient Arable Farming, an Experimental and Soil Micromorphological Study. Brit. Archaeol. Rep, Oxford, UK, 118 pp.
Macphail, R.I., Courty, M.A., Gebhardt, A., 1990. Soil micromorphological evidence of early agriculture in north-West Europe. World Archaeol. 22, 53–69. https://doi.org/10.1080/00438243.1990.9980129.
Madella, M., Lancelotti, C., 2012. Taphonomy and phytoliths: a user manual. Quat. Int. 275, 76–83. https://doi.org/10.1016/j.quaint.2011.09.008.
Madella, M., Alexandre, A., Ball, T., 2005. International code for phytolith nomenclature 1.0. Ann. Bot. Lond. 96, 253–260. https://doi.org/10.1093/aob/mci172.
Mainberger, M., 2020. Elements of an aquatic cultural landscape–a regional study from a frog's eye perspective. Archäologische Informationen 43, 309–322. https://doi.org/10.11588/ai.2020.1.81417.
Mainberger, M., Baum, T., Ebersbach, R., Gleich, P., Hesse, R., Kleinmann, A., Maier, U., Merkt, J., Million, S., Nelle, O., Stephan, E., Schlichterle, H., Vogt, R., Wick, L., 2020. New perspectives on archaeological landscapes in the south-western German alpine foreland—First results of the BeLaVi Westallgäu project. In: Settling Waterscapes in Europe: The Archaeology of Neolithic and Bronze Age Pile-Dwellings. Propylaeum, Heidelberg.
Maise, C., 2022. Löbben, Göschenen und die bronzezeitliche Besiedlung im Mittelland. Jahrbuch der Archäologie Schweiz 105, 185–191.
Martin, M., 2009. Geogene Grundgehalte (Hintergrundwerte) in den petrogeochemischen Einheiten von Baden-Württemberg. – LGRB-Informationen, 24, pp. 1–98. S.
McNeill, J.R., Winiwarter, V., 2004. Breaking the sod: humankind, history, and soil. Science 304 (5677), 1627–1629. https://doi.org/10.1126/science.1099893.
Meister, J., Krause, J., Müller-Neuhof, B., Portillo, M., Reimann, T., Schütt, B., 2017. Desert agricultural systems at EBA Jawa (Jordan): integrating archaeological and paleoenvironmental records. Quat. Int. 434, 33–50. https://doi.org/10.1016/j.quaint.2015.12.086.
Menotti, F., 2003. Cultural response to environmental change in the alpine lacustrine regions: the displacement model. Oxf. J. Archaeol. 375-396 (22), 4. https://doi.org/10.1046/j.1468-0092.2003.00194.x.
Menotti, F., 2009. Climate variations in the Circum-alpine region and their influence on Neolithic-Bronze Age lacustrine communities displacement and\or cultural adaptation. Documenta Praehistorica 36, 61–66. https://doi.org/10.4312/dp.36.3.
Miera, J.J., 2020. Ur-und frühgeschichtliche Siedlungsdynamiken zwischen Gunst-und Ungunsträumen in Südwest-deutschland. Landschaftsarchäologische Untersuchungen zur Baar und den angrenzenden Naturräumen des Schwarzwaldes und der Schwäbischen Alb. RessourcenKulturen, 10. Tübingen Univ. Press. https://doi.org/10.15496/publikation-45820.
Miera, J.J., Henkner, J., Schmidt, K., Fuchs, M., Scholten, T., Kühn, P., Knopf, T., 2019. Neolithic settlement dynamics derived from archaeological data and colluvial deposits between the Baar region and the adjacent low mountain ranges, Southwest Germany. E&G Quat. Sci. J. 68 (1), 75–93. https://doi.org/10.5194/egqsj-68-75-2019.
Morrissey, C., Langer, Höpfer, B., 2021. Bronze- und hallstattzeitliche Siedlungsspuren aus Leutkirch im Allgäu (Lkr. Ravensburg) – Neues zur Vorgeschichte des westlichen Allgäus. Fundberichte aus Baden-Württemberg 39, 103–122.
Müller, T., Oberdorfer, E., Philippi, G., 1974. Potentielle natürliche Vegetation von Baden-Württemberg. In: Veröffentlichungen der Landesstelle für Naturschutz und Landschaftspflege in Baden-Württemberg/Beiheft 6. Naturschutz und Landschaftspflege, Ludwigsburg, Landesstelle für.
Murray, A.S., Wintle, A.G., 2000. Luminescence dating of quartz using an improved single-aliquot regenerative-dose protocol. Radiat. Meas. 32, 57–73. https://doi.org/10.1016/S1350-4487(99)00253-X.
Murray, A.S., Wintle, A.G., 2003. The single aliquot regenerative dose protocol: potential for improvements in reliability. Radiat. Meas. 37, 377–381. https://doi.org/10.1016/S1350-4487(03)00053-2.
Nam, J.J., Thomas, G.O., Jaward, F.M., Steinnes, E., Gustafsson, O., Jones, K.C., 2018. PAHs in background soils from Western Europe: influence of atmospheric deposition and soil organic matter. Chemosphere 70, 9. https://doi.org/10.1016/j.chemosphere.2007.08.010.
Neumann, K., Strömberg, C., Ball, T., Albert, R.M., Vrydaghs, L., Cummings, L.C., 2019. International Committee for Phytolith Taxonomy (ICPT), International Code for Phytolith Nomenclature (ICPN) 2.0. Ann.-Bot.-London 124 (2), 189–199. https://doi.org/10.1093/aob/mcz064.
Nielsen, N.H., Kristiansen, S.M., 2014. Identifying ancient manuring: traditional phosphate vs. multi-element analysis of archaeological soil. J. Archaeol. Sci. 42, 390–398. https://doi.org/10.1016/j.jas.2013.11.013.
Nölte, J., 2003. ICP-Emissionsspektrometrie für Praktiker: Grundlagen, Methodenentwicklung, Anwendungsbeispiele, 2002. Wiley-VCH.
Novák, J., Lisá, L., Pokorný, P., Kuna, M., 2012. Charcoal analyses as an environmental tool for the study of Early Medieval sunken houses infills in Roztoky near Prague, Czech Republic. J. Archaeol. Sci. 39 (4), 808–817. https://doi.org/10.1016/j.jas.2011.06.026.
Piperno, D.R., 2006. Phytoliths: A Comprehensive Guide for Archaeologists and Palaeoecologists. Rowman Altamira.
Ponomarenko, E.V., Ershova, E.G., Stashenkov, D.A., Ponomarenko, D.S., Kochkina, A.F., 2020. Tracing land use history using a combination of soil charcoal and soil pollen analysis: an example from colluvial deposits of the Middle Volga region. J. Arch. Sci. Res. 31, 102269. https://doi.org/10.1016/j.jasrep.2020.102269.
Prøsch-Danielsen, L., 1993. Prehistoric agriculture revealed by pollen analysis, plough-marks and sediment studies at Sola, South-Western Norway. Veg. Hist. Archaeobotany 2 (4), 233–244. https://doi.org/10.1007/BF00198164.
Prost, K., Birk, J.J., Lehndorff, E., Gerlach, R., Amelung, W., 2017. Steroid biomarkers revisited–Improved source identification of faecal remains in archaeological soil material. PLoS One 12. https://doi.org/10.1371/journal.pone.0164882.
Reimer, P.J., Bard, E., Bayliss, A., Beck, J.W., Blackwell, P.G., Ramsey, C.B., Grootes, P. M., 2013. IntCal13 and Marine13 radiocarbon age calibration curves 0–50,000 years cal BP. Radiocarbon 55, 1869–1887. https://doi.org/10.2458/azu_js_rc.55.16947.
Rösch, M., Fischer, E., Kleinmann, A., Lechterbeck, J., Tserendorj, G., Wick, L., 2014. Bronzezeitliche Landnutzung im diachronen Vergleich–Fallbeispiele aus Südwestdeutschland. Ressourcen und Rohstoffe in der Bronzezeit, Arbeitsberichte zur Bodendenkmalpflege in Brandenburg, 26.
Rösch, M., Stojakowits, P., Friedmann, A., 2020. Does site elevation determine the start and intensity of human impact? Pollen evidence from southern Germany. Veg. Hist. Archaeobotany 1–14. https://doi.org/10.1007/s00334-020-00780-4.
Ryzner, K., Owczarek, P., 2020. Outline of the development of research on the impact of Neolithic settlements on the transformation on loess landscapes in southern Poland. Environ. Soc. Econ. 8 (2), 32–44. https://doi.org/10.2478/environ-2020-0010.
Scherer, S., Deckers, K., Dietel, J., Fuchs, M., Henkner, J., Höpfer, B., Junge, A., Kandeler, E., Lehndorff, E., Leinweber, P., Lomax, J., Miera, J., Poll, C., Toffolo, M. B., Knopf, T., Scholten, T., Kühn, P., 2021a. What's in a colluvial deposit? Perspectives from archaeopedology. Catena. https://doi.org/10.1016/j.catena.1245 2020.105040.
Scherer, S., Höpfer, B., Deckers, K., Fischer, E., Fuchs, M., Kandeler, E., Lechterbeck, J., Lehndorff, E., Lomax, J., Marhan, S., Marinova, E., Meister, J., Poll, C., Rahimova, H., Rösch, M., Wroth, K., Zastrow, J., Knopf, T., Scholten, T., Kühn, P., 2021b. Middle Bronze Age land use practices in the north-western alpine foreland–a multi-proxy study of colluvial deposits, archaeological features and peat bogs. SOIL 7, 269–304. https://doi.org/10.5194/soil-7-269-2021.
Scheu, S., 1992. Automated measurement of the respiratory response of soil microcompartments: active microbial biomass in earthworm faeces. Soil Biol. Biochem. 24, 1113–1118. https://doi.org/10.1016/0038-0717(92)90061-2.
Scholz, H., 2016. Bau und Werden der Allgäuer Landschaft. Schweizerbart, Stuttgart.
Schweingruber, F.H., 1990a. Microscopic Wood Anatomy: Mikroskopische Holzanatomie, Anatomie microscopique du bois. In: Birmensdorf, Eidgenössische Forschungsanstalt für Wald. Landschaft in Bern, Schnee und.
Schweingruber, F.H., 1990b. Anatomie europäischer Hölzer. Ein Atlas zur Bestimmung europäischer Baum-, Strauch- und Zwergstrauchhölzer. Anatomy of European woods/An atlas ort he identification of European trees, shrubs and dwarf shrubs, Eidgenössische Forschungsanstalt für Wald, Schnee und Landschaft in Bern.
Skujiòs, J.J., McLaren, A.D., 1968. Persistence of enzymatic activities in stored and geologically preserved soils. Enzymol. 34, 213–225.
Steinhof, A., Altenburg, M., Machts, H., 2017. Sample preparation at the Jena $^{14}$C laboratory. Radiocarbon 59, 815–830. https://doi.org/10.1017/RDC.2017.50.
Stoops, G., 2003. Guidelines for analysis and description of soil and regolith thin sections. Soil Sci. Soc. Am. J. Madison, 184p.
Stuiver, M., Polach, H.A., 1977. Discussion reporting of $^{14}$C data. Radiocarbon 19, 355–363. https://doi.org/10.1017/S0033822200003672.
Tan, Z., Wu, C., Han, Y., Zhang, Y., Mao, L., Li, D., Liu, L., Guanru, S., Yan, T., 2020. Fire history and human activity revealed through poly cyclic aromatic hydrocarbon (PAH) records at archaeological sites in the middle reaches of the Yellow River drainage basin, China. Palaeogeogr. Palaeoclimatol. Palaeoecol. 560 https://doi.org/10.1016/j.palaeo.2020.110015.
Taylor, J.P., Wilson, B., Mills, M.S., Burns, R.G., 2002. Comparison of microbial numbers and enzymatic activities in surface soils and subsoils using various techniques. Soil Biol. Biochem. 34, 387–401. https://doi.org/10.1016/S0038-0717(01)00199-7.
Teuber, S., Ahlrichs, J.J., Henkner, J., Knopf, T., Kühn, P., Scholten, T., 2017. Soil cultures–the adaptive cycle of agrarian soil use in Central Europe. Ecol. Soc. 22, 4. https://doi.org/10.5751/ES-09729-220413.
Teuber, S., Bartelheim, M., Hardenberg, R., Knopf, M., Knopf, T., Kühn, P., Schade, T., Schmidt, K., Scholten, T., 2022. Why do we need interdisciplinary cooperation with anthropologists and archaeologists in soil science? J. Plant Nutr. Soil Sci. 752–765. https://doi.org/10.1002/jpln.202200120.
Thornton, C.P., 2007. Of brass and bronze in prehistoric Southwest Asia. Metals and mines: Studies in archaeometallurgy, pp. 123–135.
Thrane, H., 1989. Danish plough-marks from the Neolithic and Bronze Age. J. Danish Archaeol. 8 (1), 111–125. https://doi.org/10.1080/0108464X.1989.10590023.
Tinner, W., Lotter, A.F., 2006. Holocene expansions of Fagus silvatica and Abies alba in Central Europe: where are we after eight decades of debate? Quat. Sci. Rev. 25 (5–6), 526–549. https://doi.org/10.1016/j.quascirev.2005.03.017.
Tinner, W., Lotter, A.F., Ammann, B., Conedera, M., Hubschmid, P., van Leeuwen, J.F., Wehrli, M., 2003. Climatic change and contemporaneous land-use phases north and south of the Alps 2300 BC to 800 AD. Quat. Sci. Rev. 22, 1447–1460. https://doi.org/10.1016/S0277-3791(03)00083-0.
Tserendorj, G., Marinova, E., Lechterbeck, J., Behling, H., Wick, L., Fischer, E., Sillmann, M., Märkle, T., Rösch, M., 2021. Intensification of agriculture in southwestern Germany between the Bronze Age and Medieval period, based on

archaeobotanical data from Baden-Württemberg. Veg. Hist. Archaeobotany 30 (1), 35–46. https://doi.org/10.1007/s00334-020-00814-x.

Tudyka, K., Bluszcz, A., Poręba, G., Miłosz, S., Adamiec, G., Kolarczyk, A., Kolb, T., Lomax, J., Fuchs, M., 2020. Increased dose rate precision in combined α and β counting in the μDose system-a probabilistic approach to data analysis. Radiat. Meas. https://doi.org/10.1016/j.radmeas.2020.106310.

Twiss, P.C., Suess, E., Smith, R.M., 1969. Morphological classification of grass phytoliths. Soil Sci. Soc. Am. J. 33, 109–115. https://doi.org/10.2136/sssaj1969.03615995003300010030x.

Van der Knaap, W.O., Van Leeuwen, J.F.N., 2001. Vegetationsgeschichte und menschlicher Einfluss in der Umgebung des Bibersees zwischen 2600 und 50 v. Chr., in: Cham-Oberwil, Hof (Kanton Zug). Befunde und Funde aus der Glockenbecherkultur und Bronzezeit, edited by: Gnepf-Horisberger, U., and Hämmerle, S., Antiqua, 33, pp. 181–194.

Varberg, J., Kaul, F., Gratuze, B., 2020. Bronze age glass and Amber evidence of bronze age long distance exchange. Adoranten 5–29.

Vogt, R., 2015. Pedologische Untersuchungen im Umfeld des jungneolithischen Fundplatzes DeI am Degersee. In: Pfahlbausiedlungen am Degersee, edited by Mainberger M., Merkt J. and Kleinmann A., Materialhefte zur Archäologie in Baden-Württemberg, p. 102.

Vogt, R., Kretschmer, I., 2019. Archaeology and agriculture: conflicts and solutions. E&G Quat. Sci. J. 68, 47–51. https://doi.org/10.5194/egqsj-68-47-2019.

Weißkopf, A., Harvey, E., Kingwell-Banham, E., Kajale, M., Mohanty, R., Fuller, D.Q., 2014. Archaeobotanical implications of phytolith assemblages from cultivated rice systems, wild rice stands and macro-regional patterns. J. Archaeol. Sci. 51, 43–53. https://doi.org/10.1016/j.jas.2013.04.026.

Whitlock, C., Larsen, C., 2001. Charcoal as a fire proxy. In: Tracking Environmental Change Using Lake Sediments. Springer, Dordrecht, pp. 75–97. https://doi.org/10.1007/0-306-47668-1_5.

Wolf, M., Lehndorff, E., Wiesenberg, G.L., Stockhausen, M., Schwark, L., Amelung, W., 2013. Towards reconstruction of past fire regimes from geochemical analysis of charcoal. Org. Geochem. 55, 11–21. https://doi.org/10.1016/j.orggeochem.2012.11.002.

Wöstehoff, L., Kindermann, K., Amelung, W., Kappenberg, A., Henselowsky, F., Lehndorff, E., 2022. Anthropogenic fire fingerprints in Late Pleistocene and Holocene sediments of Sodmein Cave, Egypt. J. Archaeol. Sci. Rep. 42, 103411. https://doi.org/10.1016/j.jasrep.2022.103411.

Würfel, F., Röpke, A., Krause, R., Lutz, J., 2010. Prähistorische Siedlungsdynamik und Landschaft in einer inneralpinen Siedlungskammer–Archäologische, geoarchäologische, archäometallurgische und archäobotanische Untersuchungen im Montafon in Vorarlberg (Österreich). Archäologisches Korrespondenzblatt 40 (4), 503–523. https://doi.org/10.11588/ak.2010.4.90176.

Young, S.D., 2013. Chemistry of heavy metals and metalloids in soils. In: Alloway, B.J. (Ed.), Heavy Metals in Soils, Environ. Pollut, 22, pp. 51–95.

Yunker, M.B., Macdonald, R.W., Vingarzan, R., Mitchell, R.H., Goyette, D., Sylvestre, S., 2002. PAHs in the Fraser River basin: a critical appraisal of PAH ratios as indicators of PAH source and composition. Org. Geochem. 33 (4), 489–515. https://doi.org/10.1016/S0146-6380(02)00002-5.

Zádorová, T., Penížek, V., Vašát, R., Žížala, D., Chuman, T., Vaněk, A., 2015. Colluvial soils as a soil organic carbon pool in different soil regions. Geoderma 253, 122–134. https://doi.org/10.1016/j.geoderma.2015.04.012.